EPRI

Coatings to Prevent Diffusion of Fission Products into Turbine Materials Used in High Temperature Gas Cooled Nuclear Electric Generating Stations

1009385

Coatings to Prevent Diffusion of Fission Products into Turbine Materials Used in High Temperature Gas Cooled Nuclear Electric Generating Stations

1009385

Technical Update, December, 2003

EPRI Project Managers

L. Loflin
J. Sharkey

EPRI • 3412 Hillview Avenue, Palo Alto, California 94304 • PO Box 10412, Palo Alto, California 94303 • USA
800.313.3774 • 650.855.2121 • askepri@epri.com • www.epri.com

DISCLAIMER OF WARRANTIES AND LIMITATION OF LIABILITIES

ORGANIZATIONS THAT PREPARED THIS DOCUMENT

University of Michigan

CA Technology Limited

This is an EPRI Technical Update report. A Technical Update report is intended as an informal report of continuing research, a meeting, or a topical study. It is not a final EPRI technical report.

ORDERING INFORMATION

Requests for copies of this report should be directed to EPRI Orders and Conferences, 1355 Willow Way, Suite 278, Concord, CA 94520. Toll-free number: 800.313.3774, press 2, or internally x5379; voice: 925.609.9169; fax: 925.609.1310.

CITATIONS

This document was prepared by

ERPI
1300 West W. T Harris Blvd.
Charlotte, NC 28262

Principal Author
D. Gandy

CA Technology Ltd
Shooters Oak School Road
West Wellow
Hampshire, United Kingdom SO51-6AR

Principal Investigator
Dr. P. Chandler

University of Michigan
3490 Wynnstone Dr.
Ann Arbor, MI 48105

Principal Investigator
Dr. G. Was

This document describes research sponsored by EPRI.

The publication is a corporate document that should be cited in the literature in the following manner:

Coatings to Prevent Diffusion of Fission Products into Turbine Materials Used in High Temperature Gas Cooled Nuclear Electric Generating Stations, EPRI, Palo Alto, CA: 2003 1009385.

ABSTRACT

This report describes EPRI activities relating to turbine blade coatings to prevent diffusion of fission products into turbine materials used in high temperature gas cooled nuclear electric generating stations. Specifically, this report describes activities that have identified candidate coatings and methodologies for evaluating the effectiveness of these coatings.

CONTENTS

INTRODUCTION AND BACKGROUND

High-temperature gas-cooled reactors (HTGRs) are being considered as options for advanced nuclear power plants. There are currently two HTGR designs being pursued. One is the Pebble Bed Modular Reactor (PBMR) under development by PBMR (Eskom), and the other is the Gas Turbine-Modular Helium Reactor (GT-MHR) under development by a consortium of organizations within the Russian Ministry of Atomic Energy and General Atomics, Framatome, and Fuji Electric.

A challenge facing the development of HTGR's is the migration of silver and cesium radionuclides from the reactor and subsequent depositing of these radionuclides onto turbine blades and internal components. The accumulation of these condensable radionuclides (plateout) in the primary coolant circuits of HTGRs has significant maintenance implications. [1] Cesium (Cs-137, Cs-134) and Silver (Ag-110m) are the dominant dose contributors to occupational exposures during normal operation. The expected plateout, especially the plateout of Cs-137, Cs-134, and Ag-110m, on the turbine of a direct-cycle MHR, such as the GT-MHR or the PBMR, will potentially produce significant radiation fields that will complicate turbine maintenance. The purpose of this effort is to provide useful information to minimize these complications and facilitate maintenance of these machines.

References:
[1] Hanson, A Review of Plateout Phenomena in Direct-Cycle HTGRs, Draft, September, 2001, EPRI Project 39063

PROJECT OBJECTIVE AND EXPECTED BENEFITS

The overall objective of this effort is to provide useful information to minimize complications from silver and cesium plateout within HTGR's and facilitate maintenance of tubines within these plants. More specifically, the goal of this effort is to identify a turbine material coating (or coatings) that helps prevent diffusion of the plated out fission products into the bulk turbine blade alloy, thereby facilitating decontamination. Furthermore, it is necessary to show convincingly that this coating or coatings can prevent the penetration of plateout activity into the bulk material under turbine operating conditions.

Coating of the turbine blades might serve to minimize penetration of the silver to the base metal and allow for easier and more effective decontamination prior to maintenance.

The objective of this interim report is to provide a status of this effort and outline the results obtained thus far.

APPROACH

The overall approach taken by the project team involved

1. Identification of candidate coatings
2. Identification of methods to measure the presence and distribution of fission product elements in contaminated specimens.
3. Determine the relative success of the coating to prevent diffusion of silver through testing.

This interim report describes the results of steps one and two above.

Initially, the project team evaluated combustion gas turbine blade and coating experience as it relates to helium gas reactor turbines. This experience included the evolution of blade materials and coatings and blade degradation mechanisms. This review also anticipated the damage mechanisms associated with Helium gas reactor turbines.

The project team identified the proposed turbine blade materials through contacts at both General Atomics and Eskom's PBMR group.

A review of candidate materials was performed based on absorption/sorptivity characteristics for cesium and silver. Surface energy data and source information from published absorption studies was reviewed. The aim will be to find materials (possibly ceramics) which have sorptivity levels 10 times lower than nickel based alloys. Three candidate coatings were identified.

A review was made of diffusion data for silver and cesium in a range of materials including nickel based alloys, other metals (e.g. Pt-Aluminide) and ceramics. The aim was to identify materials that can provide coatings and/or diffusion barriers to prevent (Silver) diffusion into the base alloy.

An assessment of possible coating methods was performed. Using the list of candidate materials, an assessment was provided of the possible coating methods that can be used. The desired coating properties and structure were defined.

Identify coating suppliers were identified who may be able to carry out work to produce the coatings for the initial simulated test samples

Methods were proposed to contaminate test specimens and measure the presence and distribution of fission product elements in contaminated specimens. Potential methods identified by the project's stakeholders were radioactive tracer techniques, gamma scanning, and vapor phase deposition.

RESULTS

Review of Combustion Gas Turbine Blade Materials and Coating Experience

Past and present gas turbine blade and coating materials experience for land-based gas turbines was investigated and documented. As a part of this review, blade materials and coating materials for gas turbines were identified, damage mechanisms were reviewed, an evolution of coatings and blade materials was provided, and an assessment was made of damage mechanisms that may be associated with HTGRs.

Identification of Candidate Coatings

Candidate coatings were identified for proposed testing. Three candidate coatings, zirconium oxide (ZrO_2), aluminum oxide (Al_2O_3) and magnesium oxide (MgO) were identified.

A review of candidate materials was performed based on absorption/sorptivity characteristics for cesium and silver. Surface energy data and source information from published absorption studies was reviewed.

A review was made of diffusion data for silver and cesium in a range of materials including nickel based alloys, other metals (e.g. Pt-Aluminide) and ceramics. The aim was to identify materials that can provide coatings and/or diffusion barriers to prevent (Silver) diffusion into the base alloy.

An assessment of possible coating methods was performed. Using the list of candidate materials, an assessment was provided of the possible coating methods that can be used. The desired coating properties and structure were defined.

Coating suppliers were identified who may be able to carry out work to produce the coatings for the initial simulated test samples

Identification of Methods to Measure Fission Product Elements

Methods were proposed to contaminate test specimens and measure the presence and distribution of fission product elements in contaminated specimens. These methods are Rutherford backscattering spectrometry, neutron activation analysis, and electron microprobe analysis.

Each of these techniques was described, along with the test procedure. A summary of advantages and disadvantages was provided. Sample preparation is discussed. A summary of test methods is provided.

FUTURE WORK

This section discusses the remaining work to accomplish the overall project objective, two issues needing resolution before a test plan is developed, and provides some of EPRI's perspective.

As stated previously, the overall approach taken by the project team involved

1. Identification of candidate coatings
2. Identification of methods to measure the presence and distribution of fission product elements in contaminated specimens.
3. Determine the relative success of the coating to prevent diffusion of silver through testing.

Step 3 in the approach, the testing phase, has yet to be accomplished. Prior to the development of a test plan, consensus will have to be reached on measurement methods and sample preparation. These two issues are discussed below.

Sample Preparation

The project team and the project stakeholders could not reach a consensus on sample preparation. This issue needs to be resolved prior to moving forward with the testing phase.

One opinion is that it is not necessary to use radioactive isotopes for testing of these coatings, which creates the requirement that all test specimens must be handled as radioactive. Rather, non-radioactive isotopes of Ag can be used to simulate diffusion through the barrier coating. Since the chemical interactions between the oxide and stable and radioactive isotopes are the same, diffusion rates will differ by the square-root of the ratio of masses. For Ag-110m and naturally occurring Ag, this results in less than a 1% difference in diffusion rate."

General Atomics, a stakeholder in the project, has stated the test specimens cannot be contaminated with aqueous solutions of the contaminant and then baked. They believe that the specimens need to be contaminated by vapor phase deposition of radioactively tagged contaminants at representative temperatures (~550 - 950 C).

To date, a test facility has not been identified that will perform vapor phase deposition of radioactively tagged contaminants. In addition, if radioactively tagged contaminants are used, this will drive up the cost of the effort.

Measurement Methods

This interim report discusses three testing methods to measure the presence and distribution of fission product elements in contaminated specimens. General Atomics, a project stakeholder, suggested a fourth method. General Atomics wishes to prepare the samples using vapor phase deposition, then use standard gamma counting techniques to quantify the total plateout before and after decontamination is performed on the samples. Although this method was proposed by General Atomics, thy also stated that both Electron microprobe analysis (EMPA) and Neutron Activation Analysis (NAA) can be useful techniques. General Atomics also stated that EMPA could be used in conjunction with standard gamma counting techniques.

EPRI Perspective –Moving Forward

Consensus from the project's main stakeholders, General Atomics and PBMR (Eskom) is an important consideration prior to embarking on a potentially costly test plan. The EPRI project team made consensus a requirement prior to any testing.

There seems to be agreement that Electron microprobe analysis (EMPA) and Neutron Activation Analysis (NAA) are useful techniques. However, a major stakeholder, General Atomics, would like to utilize standard gamma counting techniques in conjunction with vapor phase deposition.

Using the information from this report, these techniques would need to be evaluated with respect to effectiveness and feasibility. The effectiveness of Rutherford backscattering spectrometry, neutron activation analysis, and electron microprobe analysis are discussed in this document. To move forward with this effort, the effectiveness of gamma counting should be compared with other proposed techniques. In addition, the feasibility of using vapor phase deposition of radioactively tagged contaminants should be identified.

Once this is done, the project's stakeholders will be in a better position to reach consensus on a test plan, and the effectiveness of the plan.

CANDIDATE TURBINE MATERIALS

Eskom's PBMR group was contacted to identify candidate materials. The following materials were identified.

- High Pressure Turbine: Inconel 713LC rotor and stator blades
- Low Pressure Turbine: 10%Co Rotor Blades/20%Co Stator Blades
- Power Turbine: Inconel 713LC rotor and stator blades

The following designates materials for the other major turbine components:
17-4 PH Stainless Steel (Compressor Blades)

- Inconel 625 (Liners)
- Hastelloy - X (Casings)
- Inconel 718 (Rotor)
- 12%Cr-Steel (Compressor Guide vanes)
- 13%Cr-Steel (Casings)

Attachment A contains supplemental information on turbine materials as published in the EPRI report entitled, "Evaluation of Materials Issues in the PBMR and GT-MHR", October 17, 2002.

GAS TURBINE BLADE COATING EXPERIENCE

This section describes a review by David Gandy of EPRI of combustion gas turbine blade coating experience as it relates to helium gas reactor turbine operation.

The purpose this review was to examine past and present gas turbine blade and coating materials experience for land-based gas turbines and to integrate that experience into helium gas reactor turbine operation. Included in this discussion are: 1) a review of the evolution of superalloy blade materials, 2) a list of all blade, vane, and coating materials (including firing temperature) employed for gas turbines manufactured by the four major OEMs, 3) a review of damage mechanisms associated with gas-fired turbines, 4) an overview of the evolution of coatings for blade materials, 5) an assessment of turbine superalloy materials at 1600F, and finally 6) an assessment of the anticipated damage mechanisms which may be associated with the helium gas reactor turbine operation.

This review targets blade materials that are being considered for the Pebble Bed Modular Reactor (PBMR) and Gas Turbine-Modular Helium Reactor (GT-MHR) design turbines.

Evolution of Blade Materials For Gas Turbines

During the first 20 or so years of land-based gas turbine development and commercial operation (beginning with the 1950s), improvements in firing temperatures were accomplished almost solely through the development of nickel-based alloys with higher temperature strengths as depicted in Figure 1. Nickel-based alloys M-252, Nimonic 80A, and U520 were among the first blade materials employed in gas turbines and were produced via forging. Subsequent improvements in high temperature blade strength were realized with the introduction of investment casting technologies. Cast alloys such as U500 and IN738 introduced during the 1960s-70s resulted in a substantial improvement in longer term stress rupture performance over the forged superalloy blade materials.(6)

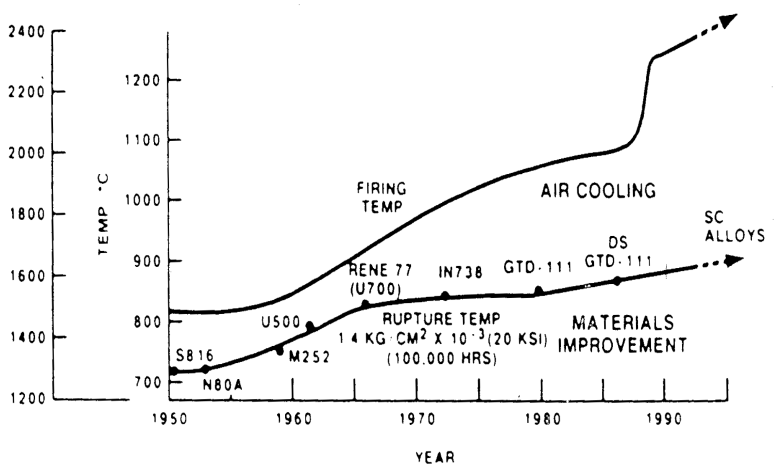

Figure 1. Gas Turbine Firing Temperature Trend Versus Blade Material Capability Versus Year Of Operation.

By the late 1960s, further improvements in alloy high temperature strength had begun to slow as a result of two important industry developments: 1) OEMs began to place a new emphasis upon the use of air-cooling to increase firing temperatures and 2) Hot corrosion of the blade alloys became the limiting factor since metal temperatures were now approaching 1600F (870C). Yet a third factor, the use of more contaminated fuels (coupled with the previous two factors) required that material developments be directed toward additional improvements in hot corrosion resistance and the use of corrosion resistant coatings.

By the early 1980s, a swing in emphasis back toward the development of stronger alloys began to occur. The swing was an effort on the part of OEMs to fill part of the need for machine uprating. By the end of this decade, high strength directionally solidified airfoils were introduced in several gas turbine designs and firing temperatures were seen to improve considerably. The 1990s have seen an additional advancement in alloy strength with the introduction of single crystal nickel-based alloys. (1)

On an average turbine blade material temperature capability has increased an average of roughly 20F per year since 1950. The importance of this increase is appreciated by the fact that an increase of 100F in turbine firing temperature will provide a corresponding increase of 10-13 percent in megawatt output and 2-4 percent improvement in simple cycle efficiency. (2)

Superalloy blade material evolution has been dictated by a delicate balance of requirements in strength, hot corrosion resistance, oxidation resistance, elimination of a deleterious sigma phase formation, and in early vintage GTs by forgeability. Cast superalloys were (and continue to be used in cooler rows of the turbine) employed almost exclusively in GTs during the late 1960s to the mid-1980s. Increases in turbine inlet temperatures which mandate higher temperature strengths, eventually led to the development of ***directionally solidified*** (DS) and single crystal blade alloys.

In combustion turbines, the creep-rupture life of conventionally cast (equiaxed) superalloys is generally limited by cracking at the grain boundaries normal to the direction of centrifugal loading. To eliminate creep cracking along this direction, the concept of directionally solidification was introduced. In this approach, all grains within a blade are aligned parallel to the loading direction. Significant improvements in creep strength (1 to 2 percent strain) and rupture life were realized with this new development. Other improvements associated with directional solidification included resistance to thermal fatigue, crack growth, and oxidation as compared to the castable versions of superalloys.

Earlier DS alloys closely resembled the compositions of the advanced equiaxed superalloys. Soon it was discovered that the use of the DS method, along with additions of hafnium, made it possible to produce considerable improvements in rupture strength. Additionally, reducing the Ti/Al ratio and adding Ta assisted in optimization of the oxidation resistance of the alloys.

Several OEMs use DS first stage blades (buckets) including the MS7001F and MS9001, along with the uprated MS3002 and MS5002 models produced by General Electric. GE employs DS GTD111 for these machines. Compared with the equiaxed counterpart to DS GTD111, the DS material offers improved creep life, impact strength (by over 33%) and thermal fatigue resistance (by greater that 10X). Alstom and Siemens-Westinghouse offer comparable DS materials in their advanced machines also. Table 1 provides a comprehensive overview of the primary turbine alloys for vanes and blades, along with the corresponding coatings employed for each.

Single crystal superalloys were first introduced commercially in an aircraft engine in 1982 by Pratt & Whitney. With this technology, grain boundaries are completely eliminated and the entire blade becomes one grain. In recent years, all major aircraft manufactures have introduced SC alloys. Solar Industrial Turbines produced the first land based turbine in 1990 which employed the SC blade technology blade. Since then, both Siemens (V84/94.3A)and GE (9H) have introduced SC alloys for blading (See Table 1). The V84.3A Siemens engine, which was placed in service in 1997, is a 170MW engine and utilizes SC alloys in both rows 1 and 2. The GE 7H/9H engines introduced single crystal technology in 1998. (4)

Siemens-Westinghouse is also reported to have developed a SC alloy, but has not introduced the alloy to its fleet. Pallotta reports the current DS alloy produced by Siemens-Westinghouse provides a temperature capability of more than 50% greater than the IN738LC, while the SC alloy has a capability of 100% or greater. (9)

Single crystal designs offer improved flexibility in alloy design and an increase in temperature capability. OEMs are beginning to move toward single crystal design over DS blades due to following reasons:

- The DS process produces large MC-type carbides in some alloys. Such carbides may often be precracked and initiate fatigue cracks under cyclic loading conditions.

- If the grain boundaries in a DS alloy are not aligned perfectly along the solidification direction, creep cracks may initiate at the boundaries where they intersect the free surface.
- The removal of grain boundary strengthening elements such as C, B, Zr, and Hf can improve fatigue properties by elimination of the MC-type carbides. Further improvement in creep resistance could be realized due the increase in melting temperature and elimination of the melting-point depressant elements. An improvement in melting point, permits solutioning of large levels of coarse gamma prime with later precipitates into fine gamma prime, providing an opportunity for the alloy to reach its full strength potential.
- More flexibility in alloying can be achieved in the absence of grain boundaries. This results in a better balance of creep-rupture strength and oxidation/hot corrosion resistance.
- Improved castability can be realized from the development of leaner (less alloying elements) alloys.

Improvements in the area of single crystal technology are necessary for these alloys to continue to gain wider usage in gas turbine blades. A few of the desired improvements are listed below.

- SC alloys do not provide sufficient hot corrosion due to the reduce levels of Cr associated with the alloys.
- Large, rapid cooling rates (7C/mm) are required during the casting process for large blades. When insufficient gradients are not realized, casting defects such as equiaxed grains, freckles, or low angle boundaries can be produced. Furthermore, porosity and reduced fatigue strength may result.
- Low production rates are common, improved casting output is warranted. (1)

Of these improvements, the latter appears to have greater influence at this particular point in time. High reject rates associated with casting of SC alloys equates to higher costs. These costs are passed along to the user.

Table 1--Combustion Turbine Alloys and Coatings for Hot Section Blading. (1)

OEM	Model	Firing Temperature	Vanes	Blades	Coatings
Alstom (ABB)	11N2		IN939	IN738LC	NiCrA1Y (some rows)
	GT24/GT 26		DS CM247LC(R1)/MarM24 7LC(R2&3)/IN738) (R4&5)	DS CM247LC(R1-3) MarM-247LC(R4&5)	TBC(RIV)/NiCrA1Y+Si(R2-4 B&V) Uncoated (R5V), Chromized (R5B)
GE	6B	2010F	FSX-414 (All Stages)	U500	
	6F/FA	2300F	FSX-414(R1)/GTD222(R2&R 3)		
	7B	1840F	FSX-414 (All Stages)	IN738(R1) U500(R2) U500(R3)	CrAl, DifAl, MCrAlY, PTAl, SiAl (All Bucket Rows)
	7/9 EA	2010F	FSX-414 (All Stages)	GTD111(R1) IN738(R2) U-500(R3)	RT22→GT29-In+(R1B)
	7/9 FA	2300F (1260C)	FSX-414(R1)/GTD222(R2&3)	DS GTD111(R1) GTD111 (R2&3)	GT33-In(R1)/GT29-In+(R2)/Chromized (R3)
	7H	2600 (1425F)	SC Rene N5 (R1)/DS GTD222 (R2, 3 & 4)	**SC** Rene N5 (R1) DS GTD111 (R2, 3 & 4)	TBC (R1&2 B&V) All others GT33
Siemens	V84/94.2		IN939 (All 4 Rows)	IN738LC (R1, 2 & 3) IN792 (R4)	CoNiCrA1Y+Si(some rows)
	V84/94.3 A		(SC)PWA1483 (R1&2)/IN939 (R3&4)	**SC** PWA1483 (R1&2)	TBC(EB-PVD) (R1B)/McrA1Y+Re

S-W	501AA		X45 (R1) or ECY768	U520 (R1 & R2)	
	501B		X45 (R1) or ECY768	U520 (R1 & R2)	
	501D5/D 5A		ECY-768 (R1&3)/X-45 (R2&4)	IN738 (R1) U-520 (R2, 3&4)	TBC (partial on R1V)/McrA1Y (some blade rows)
	501F	2300F (1260C)	ECY-768 (R1, 2 & 3)/X-45 (R4)	IN738LC (Four Rows)	TBC (R1 B&V)/McrA1Y (R2&3B)/SermalloyJ (R4B)*
MHI	501G	2600F (1425F)	IN939 (Four Rows)	DS MM002 (R1&2) EA CM247 (R3&4) Or DS CM 247 (R1&2)	TCB (EB-PVD) (R1 B&V) TCB (R2 B&V) McrA1Y (R3 B&V)
	501/701 D/DA 501/701F 701G	2600F (1425F)	Similar to S-W	Similar to S-W	Similar to S-W

Rene N5: 7.5Co, 7Cr, 1.5Mo, 5W, 3Re, 6.5Ta, 6.2Al, 0.05C, 0.2B, 0.01Y
SCPWA 1483: 12%Cr Alloy similar to INCO792
GT29: CoCrA1Y; GT29+: CoCrA1Y+Diffusion Aluminide Top Coat
GT33: McrA1Y with Improved Oxidation Resistance
*TBC with McrA1Y bond coat for Row 1 Blade & Vane (Plasma Sprayed)
+TBC with McrA1Y bond coat for Rows 1 and 2 Blades & Vanes

Degradation Mechanisms Associated With Gas-Fired Turbines (8)

Hot Corrosion

Hot Corrosion is a form of environmental attack which occurs due to the presence of *contaminants* (usually sulfates) in the operating gas medium of a combustion turbine. Blades and vanes located in the hot-gas path in the turbine section are subject to this combined oxidation-sulfidation phenomenon. If the operating gas medium is relatively clean, hot corrosion is generally not a problem.

Three basic types of hot corrosion attack have been documented in operating gas turbines. (Ref 8). The first occurs over a temperature range of 1200 to 1300F (650C to 705C). Here a *layer-type corrosion* occurs and is characterized by an uneven scale/metal interface along with the absence of sub-scale sulfides. As the temperature is increased to above 1400F (760C), **a *non-layer type* (Type I*) corrosion*** is observed. This form of corrosion is characterized by a smooth scale/metal interface and a continuous, uniform precipitate-depleted zone containing individual sulfide particles beneath the scale.

A transition from the first form of hot corrosion to the second occurs between 1300F and 1400F (705 and 760C). Within this temperature range, an uneven scale/metal interface is observed that contains intermittent pockets of subscale precipitate-depleted zones and sulfides. Together the layer-type corrosion and the transitional corrosion are referred to as ***Type II corrosion*** or low temperature corrosion. Figure 2 provides a schematic representation of the two types of corrosion along with an oxidation curve.

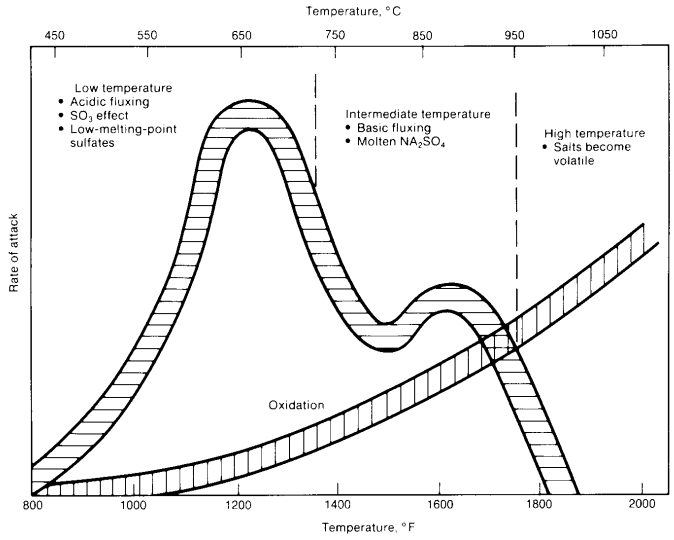

Figure 2. Illustration of the variation in corrosion rate with temperature due to changes in hot-corrosion mechanism.

In practice, chromia-type scales are more protective than alumina-type scales, particularly in the lower temperature form of hot corrosion. However, higher levels of chromium may be required to maintain a chromia layer under hot corrosion

conditions. It is for this reason, cobalt alloys (with a higher chromium content) outperform nickel-based alloys in hot corrosion.

Oxidation

Oxidation takes over as the primary corrosion mechanism above 1700F. Blade metal wastage can be caused by oxidation and increases with temperature and the level of contaminants in the combustion gases. Minute quantities of contaminants such as sodium, potassium, lead, or vanadium can have a dramatic effect on bucket life. Contaminants may be associated with one of three sources:

- Air—such as onsite construction, fertilizers, nearby industrial plants, salt water environment, ineffective air filters, etc.
- Fuel—either as delivered or as a result of improper handling of the fuel during transporation
- Steam or water—such as Nox control, power augmentation, compressor cleaning, or evaporative cooling.

In practice, contamination results of non-fuel type sources over one-half the time. Foster (3) states that pound for pound, a contaminant is equally harmful from any of the three sources described.

Creep Damage

Failures by creep can occur in hot-section components as a result of continuous exposure to high stresses and temperatures. Superalloy turbine blades are designed on a basis of a given stress to cause rupture or a given percent of elongation over a specified time. This results in a specified design life period. Premature failures in superalloy components are often caused by unanticipated excursions in temperature or stress and by contributing corrosion factors. Predicting long term performance of a blade material based on short time test data has been shown as a contributing factor in many blade creep failures. Extrapolation of short time data is occasionally optimistic and does not take into account microstructural degradation phenomenon such as coarsening of gamma prime, grain boundary carbides, or the formation of deleterious phases such as sigma. (8)

Creep failure may occur as a result of continuous or cyclic exposure to stresses and temperatures encountered in hot section gas turbine components. An accumulation of damage along the grain boundaries in the form of microscopic voids describes the creep phenomenon. Linking of the voids can lead to micro-cracks and eventually to critical crack-size flaws. It is for this reason that blade manufacturers have moved toward directionally solidified and now single crystal alloys.

Blades and other hot section components are exposed to regenerative heat treatments to restore high temperature properties after a given time of operation. This is particularly true of the more common conventionally cast (equiaxed structure) components were creep damage and other grain boundary embrittlement mechanisms can be eliminated or reduced. Regenerative hot isostatic processing methods have been perfected by OEMs/repair vendors to restore blade properties to near new. Such

regenerative practices are applied to blades following coating stripping and prior to coating reapplication.

One of the more commonly used methods for comparing the long term performance of blade superalloys under creep conditions is via the use of stress rupture testing. In this test, test specimens from the blade are loaded under constant stress conditions and tested until failure. The results are several tests are then plotted on a Larson-Miller curve which takes into account stress, temperature, and time to failure. An example comparing several earlier blade alloys is shown in Figure 3. The significance of this plot is that it can be readily used to compare one blade alloy to another for a variety of stress and temperature conditions. In a latter section of this document, blade material rupture strengths are compared at 1600F which is near the operating temperature of both the Russian and South African turbine blade operating temperatures. (8)

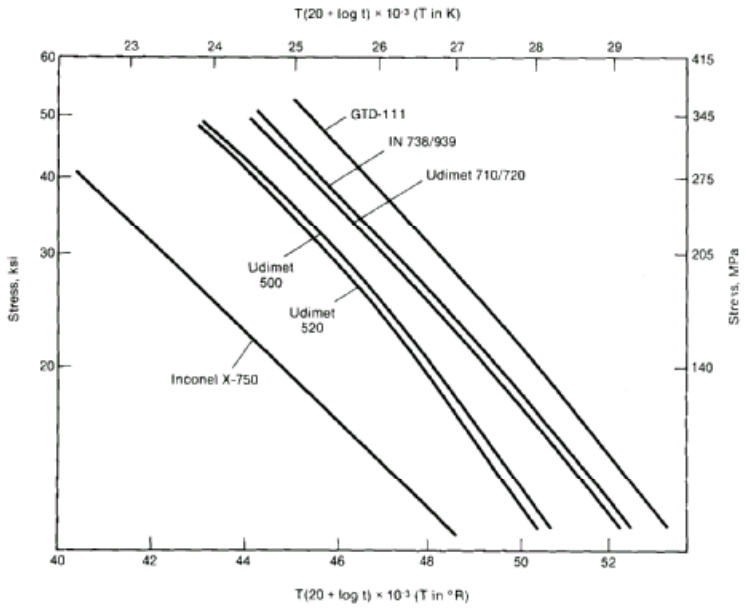

Figure 3. Larson-Miller stress-rupture plots for blade alloys

Fatigue Damage

Fatigue failures in gas turbine blades occur as the result of repetitive or fluctuating stresses at levels generally much lower than the tensile strength of the blade. Fatigue, unlike creep, is *not strongly influenced* by temperature and may occur in hot- or cold-section components. Fatigue failures may be characterized as either low or high cycle failures, depending upon the frequency of the loading.

Low cycle fatigue (LCF) in blades occurs (in most cases) as the result of stresses applied once per engine cycle, such as those resulting from differential thermal expansion during start up and shutdown. Stress levels approaching the yield stress of the superalloy are required to initiate and propagate cracking under such conditions. Conversely, the occurrence of high cycle fatigue is associated with higher frequency resonant conditions. Coupled with the applied steady and low-frequency transient

cycle stress conditions, the resonance of a component becomes an important factor and acts to increase the stresses on a component or part.

Damage under low cycle fatigue conditions is dependant upon the temperature range over which it occurs and may accumulate through plastic deformation or by a combination of plastic and creep deformation (at higher temperatures only). Cracks which occur at high temperature via LCF appear similar to creep cracks. The cracks exhibit an intergranular fracture path and contain intergranular voids. LCF cracks can be distinguished from creep cracks by 1) their locations in areas where steady-state stresses are low, 2) their larger appearance, and 3) more numerous voids which are present. (8)

Elastic deformation predominates in all temperature regimes where high cycle fatigue occurs. Such cracks initiate and propagate along transgranular paths and provide a characteristically smooth surface appearance.

Blade cracking associated with either LCF or HCF is rare in gas turbine operation. If fatigue cracking does occur, it is usually associated with a breakdown in the coating.

Creep-Fatigue Interaction

Under continuous cycling conditions, pure low cycle fatigue is rare, because during machine operation components are frequently held at high temperatures between cycles. If operating conditions are held below the creep temperature range, a pure low cycle fatigue situation may apply. However, the more common situation for blade materials to experience is where the blade operates within the creep range. At such temperatures, damage contribution due to stress relaxation must be also taken into account. Furthermore, independent variations in strain and temperature may be involved. In the laboratory, such conditions are extremely difficult to replicate. Isothermal LCF tests are more likely to be used in the laboratory and may fail to replicate the independent strain or temperature variations.

Data on creep-fatigue interactions for blades or vane alloys for land-based gas turbines is limited except for the more commonly used alloys such as IN738 or GTD111. As newer, more advanced, blade alloys enter the market place, it becomes more difficult to predict or understand the creep-fatigue interactions that the material may experience. The practice most often employed by blade designers is to conduct isothermal fatigue tests at the maximum operating temperature to define the worst case behavior of the blade alloy. (8)

Service-Induced Damage

Design of gas turbine blades and other high temperature components is based upon extrapolation of short-term laboratory data to project long term service experience. Errors in life prediction by the OEM are usually rare; however, a few instances have been observed over the years where failures have occurred at considerably shorter intervals than predicted by short-term testing. One example of such an error which resulted in premature failure is that associated with the creep performance of the blade alloy Udimet 700. Short-term stress rupture properties of this alloy suggested the

alloy should provide adequate performance for the designed service (>48,000 hours). However, when placed in service, a brittle sigma phase was generated in the blade alloy resulting in failures in fewer than 10,000 hours service.

This example highlights the need for blade designers to consider a variety of factors which may effect service life. In-service damage can result from a combination of many mechanisms and therefore designers must consider collectively all materials properties for that alloy. (8)

The Evolution Of Coatings

The earliest coatings employed by the gas turbine industry were *diffusion aluminides*. Aluminides are applied by *pack cementation* and are used to primarily protect against oxidation. Increasing evidence of Type I hot corrosion during the late 1960s lead to the development of platinum-aluminide coatings such as RT22 and RT44. These coatings specifically targeted improved resistance to Type I corrosion, but also met rigorous blade coating demands associated with thermal cycling during operation. (1)

By the mid-1970s, Type II hot corrosion (low temperature) had become a common industry problem and improved coatings were warranted. The improved coatings, based on CoCrAlY, made use of the addition of chromium to the aluminide. Chromium could not be readily added to the coating composition and then applied via pack cementation, As a result, alternative *overlay-type* coating technologies such as electron beam physical vapor deposition (EB-PVD) were utilized to apply the chromium enriched aluminides.

Overlay-type coatings in general are based upon the composition MCrAlY, where M can be nickel or cobalt or a combination of the two. Type I (high temperature) hot corrosion depends on Al_2O_3 form protection, while Type II (low temperature) hot corrosion depends on Cr_2O_3 for protection. Coatings which exhibit the greatest high temperature hot corrosion performance rely on a high aluminum (11%) content and a low chromium (<23%) content. Coatings for Type I corrosion protection employ >30% chromium and are low in aluminum. Other minor additions of elements such as silicon, hafnium, tantalum, and platinum are added to these coatings to improve corrosion and spalling resistance.

Initially CoCrAlY compositions were developed to target the Type II corrosion and thermal cycling conditions. To further improve the chromium/aluminum ratio which is important to control corrosion or oxidation performance, nickel was added to the CoCrAlY forming a new class of coatings NiCoCrAlY. This class of coatings were applied by vacuum plasma spray methods. Many current overlay-type coatings contain a double layer consisting of an outer aluminide layer for oxidation resistance and an inner layer of CoCrAlY or NiCoCrAlY balanced for Type I and II hot corrosion resistance.

Coatings employed by General Electric (3) over the past three decades include the following:

Coating		Years In Use	Type
PtAl	Platinum-aluminide	1974-present	Plate & diffusion pack
GT29	CoCrAlY	1984-88	LP plasma spray
GT29+	CoCrAlY with overlay Pt-Al coat	1990-present	LP plasma spray & diffusion pack
GT33	NiCoCrAlY	1994-present	LP plasma spray
GT33+	NiCoCrAlY with overlay Pt-Al coat	1994-present	LP plasma spray & diffusion pack

Platinum-Aluminides (PtAl) is commonly applied via a platinum electroplate followed by a diffusion pack of the aluminide. Pt-Aluminides provide good oxidation resistance, but lacks somewhat in corrosion resistance. The coatings have demonstrated a tendency to craze crack with thermal cycling.

GT29 is a patented CoCrAlY coating that is applied with plasma spray. It was introduced in 1983 on certain radial-cooled buckets and then later on other style buckets. According to GE, the GT29 coating possesses nearly twice the corrosion resistance of conventional Pt-Aluminides. GT29 does not exhibit sufficient oxidation resistance for the more recent higher temperature machines.

GT29+ was introduced to provide comparable oxidation resistance to the Pt-Aluminides while maintaining the corrosion performance of the GT29 coatings. The GT29+ coating is essentially a GT29 which has been topcoated with a diffused aluminide topcoat layer. The coating does have a propensity to craze crack but, unlike the Pt-Aluminides, the cracking does not reach the blade substrate. The cracking is blunted by the GT29 inner layer. In 1989, GT29+ replaced all GT29 coatings on air-cooled bucket designs.

GT33 is a NiCoCrAlY coating which provides significantly improved ductility over the GT29 coating. This coating is applied using plasma spray and represents essentially a 4^{th} generation of coatings. GT33+ is a NiCoCrAlY with a Pt-Aluminide top coating which represents the 5^{th} generation of coatings. This coating is also applied with plasma spray and provides excellent resistance to thermal cycling and oxidation conditions.

Thermal barrier coatings (TBCs) were introduced for gas turbine blade/vane protection as turbine firing temperatures exceeded 1120C (2050F). The function of a thermal barrier coatings is to retard the conduction of heat from the combustion gas to the internal cooling air. As a result, the cooling air required is reduced or the turbine inlet temperature can be increased for a given metal substrate. TBCs typically consist of a porous layer of zirconium oxide (ZrO_2) which is stabilized with yttria and magnesium oxide. Most TBCs are applied using plasma spray methods over a McrAlY bond coat. Bond layer thickness is on the order of 75-125 microns while the oxide layer is 125-375 microns thick. TBCs may decrease the temperature of the blade by as much as 100C (180F). TBCs are also known to smooth out hot spots and reduce thermal fatigue stresses.

Considerable variation in blade oxidation/corrosion life has been observed by industry and is usually associated with the level of contamination experienced. GE reports

their GT29 coated radial cooled first stage buckets (blades) have exhibited service lives ranging from 40,000 to 53,000 hours. GT29+ and Pt-aluminide coatings see significantly longer lives of between 58,000 and 70,000 hours. GE recommends that blades be thoroughly inspected at 24,000 hours (during a normal hot gas path inspection) and then boresonically tested at least every 8000 hours thereafter.(3)

Industry practice associated with non-TBC type coatings (Pt-aluminides and McrAlYs) is to strip the coating via chemical dipping after 24,000 hours. Coatings are routinely removed by repair vendors and OEMs via a combination of HF/HCl dipping and then restored with a new coating. Removal and restoration is warranted as blade coatings lose their ability to protect the blade from degradation by corrosion and/or oxidation. Blade coatings must maintain a minimum level (usually greater than 5-6%) of aluminum to maintain its protective capabilities. Stripping of the coating is normally limited to no more than two stripping sequences due to the fact that the stripping media is very aggressive and will attack the substrate blade resulting in wall thinning. Hence, blades must be discarded and replaced after 2-3 stripping sequences. Recent industry experience with newer machines has shown that coating life for higher firing temperature machines may be on the order of one-half that of the earlier MCrAlY type coatings.

Review Of Blade Performance For Operation At 1650F

As discussed earlier, superalloy evolution is dictated by a delicate balance of requirements in strength (tensile, fatigue, and creep), hot corrosion resistance, oxidation resistance, ductility and toughness, and the elimination of a deleterious sigma phase formation. For the new HGRT designs, two of these items, hot corrosion and oxidation, do not appear to be factors. Under helium operating conditions, the two damage mechanisms are of little concern since both are associated only with gas-fired operation. Additionally, sigma phase formation no longer appears to be an issue as casting and heat treating methods have improved. As a result, the following discussion will focus solely upon the superalloy strength and ductility near the anticipated blade operating temperature.

The following table provides mechanical property data for all past and current blade materials at 1600F[1] which is similar to the operating temperatures of the PBMR and GT-MHR turbines. Specific data includes tensile and yield strength data, elongation, and creep rupture strength at 1600F. Fatigue and toughness data have not been included. Property data for these alloys is compared directly to mechanical property information supplied for both the PBMR and GT-MHR turbine designs. As shown, the advanced DS and SC alloys provide remarkable increases in tensile and creep rupture strength when compared to the earlier equiaxed blade materials. As a result, either of the materials selected appear to meet the 1650F design temperature requirements.

It is also important to point out that the design of the PBMR and GT-MHR turbines may dictate the use of higher strength alloys for blades at the 1650F temperature.

[1] Data is typically reported in increments of 200F (ie., 1400F, 1600F, and 1800F). As a result, the temperature value (1600F) closest to the helium temperature was selected for comparison.

Blade design includes a variety of factors such as air or steam cooling, blade strength, coatings employed, pressure and temperature exposure, etc.

	Blade Strength @ 1600F			**1000-hrs Rupture Strength (ksi) @ 1600F**
	0.2% Yield Strength (ksi)	**Ultimate Tensile Strength (ksi)**	**% Elongation in 2 in.**	
Equiaxed Blade Alloys				
• U520	75(520)	75 (520)	20	22 (150)
• U500	87(603)	96(665)	9	24 (165)
• IN738LC	80(554)	112(776)	11	32 (220)
• IN939	58(401)	93(645)	7	
• IN792	96(665)	122(845)	8	38 (260)
• GTD111 EA	63(437)	92(638)	7	35 (240)
• MAR-M 247LC	97(670)	116(800)	5	42 (290)
Directionally Solidified Blade Alloys				
• GTD111 DS	77(533)	102(709)	12	35 (240)
• CM247LC DS[2]	122(839)	126(870)	10.5	23(160)[1]
• MM002 DS	80(554)	120(831)	7	44 (305)
Single Crystal Blade Alloys				
• PWA1483 SC				
• Rene N5 SC				
Blade Materials Under Consideration **For PBMR and GT-MHR Designs**				
• CM186 LC DS (SA/Alstom)[3]	123(850)	147 (1020)	10	43(300)
• CMSX-4 SC (SA/Alstom)	NA	NA	NA	29(200)[1]
• CNK-8M (Russian/Siemens)				
• ZhS6K (Russsian/Siemens)				
• ChS120-M SC (Rus./Siemens)				

1 Data was reported at 1800F (982C) since materials were designed for higher temperature operation.
2 Data reported at 1560F (850C).
3 CM186LC DS has been selected as the blade alloy by Alstom/ESKOM.

Anticipated Damage Mechanisms Associated With Helium Gas Reactor Turbine Operation

The following table compares the damage mechanisms associated with a conventional land-based gas turbine versus those anticipated for the helium gas reactor turbine.

Damage Mechanism	Conventional Land-Based Gas Turbine	Helium Gas Reactor Turbine Operating @ 1650F
Type I Hot Corrosion	Yes (requires coating)	No
Type II Hot Corrosion	Yes (requires coating)	No
Oxidation	Yes (requires coating)	No
Creep	Yes	Yes
Fatigue	Yes	Yes
Creep-Fatigue	Yes	Yes
In-service Induced Damage	Yes	Yes
Superalloy Blade Embrittlement • Cesium isotope • Silver isotope	 No No	 Unknown Unknown

This table points to the fact that turbine blades operating in a helium medium experience must meet similar requirements to those of conventional gas turbine blades operating in a combustion medium with the exception of hot corrosion and oxidation requirements. Additionally, blade embrittlement issues associated with the plate-out of cesium and silver isotopes is an unknown which must be taken into consideration.

Key Observations on Gas Turbine Blade Coating Experience

- Hot corrosion issues are not a concern for helium gas reactor turbine operation since contaminants typically associated with combustion gases are not present.
- Oxidation also does not appear to be an issue, again since the turbine operates in an inert helium environment.
- One issue which should be addressed by designers is the potential embrittlement of the blade superalloy material associated with the plate-out of cesium- and silver isotopes. Key variables appear to be deposition rate and the elemental nature of these isotopes.
- Plate-out may effect other turbine components beyond just the blading material. Vanes, discs, rotor, and casings should be evaluated on an individual basis for operation under plate-out conditions.
- Selection of the blade alloy should be based upon a review of all mechanical properties: tensile, creep, fatigue, creep-fatigue, toughness, and resistance to embrittlement.

References

1. S.T. Scheirer and R. Viswanathan, Evolution of Hot Section Materials Technology, ASM Materials Solution Conference & Exposition, Energy Utilities Program, St. Louis, MO, October 9-11, 2000.

2. P.W. Schilke, A.D. Foster, and J.J. Pepe, Advanced Gas Turbine Materials and Coatings, GE Reference Library Publication GER-3569.

3. Allan D. Foster, First-Stage Bucket Coatings—Description, Life, and Refurbishment, GE Reference Library Publication GER-3632

4. D. Gandy, Status of Weld Repair Technology for Nickel-Based Superalloy Gas Turbine Blading, EPRI Report TR-108272.

5. D. Gandy, R. Viswanathan, and J. Scheibel, Assessment of Laser Welding Process for Superalloy Gas Turbine Blade Welding, EPRI Report TR-113748,

6. C. Sims, N. Stoloff, and W. Hagel, Superalloys II, John Wiley & Sons Publishers,

7. EPRI Hot Section Component Repair Workshop, EPRI Combustion Turbine Center, September 15-16, 1992.

8. R. Viswanathan, Damage Mechanisms and Life Assessment of High – Temperature Components, ASM International, Metals Park Ohio, 1989, Section 9.

9. A. Pallotta, “Trends in Combustion Materials and Coatings—Westinghouse’s Perspective:, Proceedings of the Steam and Combustion Turbine Materials. 10/92, EPRI Report TR-102954, S.T. Scheirer and R. Viswanathan, Eds. 1993

10. D. Tillack, Presentation to Edison Electric Institute Materials & Process Task Force, April 1993.

IDENTIFICATION OF CANDIDATE COATINGS

This section discusses candidate coatings evaluated by Dr. Peter Chandler to inhibit plate-out onto HTGR turbine blades. This section provides a list of these candidate ceramic coating materials and coating processes and suppliers for turbine blades used in High Temperature Gas-cooled Reactors (HTGR's).

The principal role for these coatings is to provide a barrier to 'plate-out' of radio-active species of Ag (silver) and Cs (caesium). It is assumed that the use of the ceramic coating will either inhibit plate-out of these active elements and/or limit diffusion of these species into the base material. Furthermore, it will also be able to strip the ceramic coating during turbine maintenance so as to remove any radio-active material.

The turbine blade material is assumed to be Inconel 713 or other nickel based alloy and have a maximum operating temperature of 800°C –900°C.

Summary of Candidate Coatings

The lack of data on either the surface energy of ceramic coatings or on the interaction (ie adsorption-sorption and diffusion) of silver and caesium with ceramic materials has made this work very difficult. While these issues will be addressed elsewhere, a more pragmatic approach to the selection of candidate ceramic materials has had to be adopted. This study, based upon work on 'conventional' gas turbines, has identified those ceramics that have the potential to survive the service conditions experienced by the turbine blades.

To date, only one ceramic material has been successfully applied to operating gas turbine blades. This is a zirconium oxide based material. Although this coating is used as thermal barrier, a number of features arising from its development are pertinent to this present study. For example, it was found that the thermal mis-match between the turbine blade alloy and the ceramic was critical in determining the durability of the coating in service.

Based upon the above, it has been possible to identify a number of ceramics that could provide durable coatings for this application. Apart from zirconium oxide (ZrO_2) these include aluminium oxide (Al_2O_3) and magnesium oxide (MgO).

Similarly, only a small number of coating processes are suitable for this work and even fewer have been successfully used to deposit coatings onto turbine blades. As far as coating processes are concerned, combinations of electron beam Physical Vapour Deposition (eb-PVD), Vacuum Plasma or Low Pressure Plasma Spraying (VPS or

LPPS) and aluminising by Chemical Vapour Deposition(CVD) are the main candidates.

Finally, potential coating suppliers have been identified both in Europe and the USA.

Background

To date only one ceramic material (based upon the zirconium oxide system) has been applied to rotating turbine components. These coatings were originally developed for flight, aero-engine applications but in the last few years have begun to be exploited within industrial gas turbines as well. The zirconia based coatings were developed to provide part of a thermal barrier system which is used to reduce the operating temperature of the blades and thus increase blade life. They are generally applied over an MCrAlY (where M=Co, Cr, Ni) base coating. This coating provides resistance against surface oxidation/sulphidation and can also provide an aid to bonding of the ceramic layer. It is important to note that the effectiveness of the thermal barrier system relies upon the use of blade cooling which enables a thermal gradient across the coating to be maintained.

It is important to note that zirconia was selected for two main reasons. The low thermal conductivity of this material makes it particularly attractive as a thermal barrier but it also has a relatively high coefficient of expansion. This property has been found to be critical to the durability of ceramic coatings on rotating, turbine components.

In the case of HTGR turbines the thermal barrier aspects are not really relevant and so ceramics having higher thermal conductivity can be included. The next section will review some of the selection criteria that should be considered. The main process technologies used to deposit these coatings will be reviewed in section 4 and potential coating suppliers are presented in section 5.

Selection Criteria for Candidate Ceramic Coatings

General

There are four main selection criteria for ceramic coatings to be in this application. These are:

Ideally the selection of candidate ceramics would have been made by using data on their surface characteristics. The surface energy of the ceramic will influence the reactivity of the silver and caesium species, their sticking coefficient, adsorption characteristics, nucleation and growth and desorption characteristics. Similarly knowledge of sorptivity and diffusion would also aid the selection process. However, there appears to be very little data available in the published literature. (This conclusion is supported by Hanson, General Atomics).

An alternative strategy has thus been adopted based upon properties of a range of ceramic materials that will allow them to survive within a gas turbine especially on turbine blades. This approach assumes that the lower surface energy and reactivity of ceramics will represent an improvement over un-coated nickel based alloys. Furthermore, it will also be able to strip the ceramic coating during maintenance thus allowing for the disposal of any contained active silver or caesium.

There are numerous ceramic materials that are commonly available which are used in a wide range of applications. Many of these commonly available materials have also been applied as coatings. Generally ceramic materials have strengths of less than 1/5 of super-alloys up to 700°C and even at 1000°C are still considerably lower. Ceramics are also brittle and so sensitive to cracking.

The thermal shock resistance of ceramics is thus an important consideration. Materials such as zirconia used in high temperature applications have very good thermal shock resistance. But while alumina is good ceramics such as chromium oxide have only moderate resistance.

Another important factor is the phase stability of the ceramic material with temperature. Phase changes in ceramic materials can result in volume change and cracking on cooling leading to rapid coating failure. Finally, the effect of stress on coatings can be a major factor in coating failure in service. These aspects are discussed in more detail below. For example, pure zirconium oxide phase change at about 800°C. Below this the monocline phase is stable while above the stable phase is tetragonal. Since there is a large density difference between the two phases (monocline = 5.56 g/cc and tetragonal = 6.10g/cc) a large, destructive volume change (10%) can be expected. This problem can be overcome by stabilising a particular phase over the operating temperature range. For zirconia, additions of 3-15% CaO, MgO, CeO, Y_2O_3 can stabilise the cubic structure.

Stresses in Coatings

The effect of stress on ceramic coatings is a critical area for consideration for turbine applications. There are four sources of stress that need to be considered:

- those produced during processing (residual stresses)
- those due to thermal gradients
- those due to expansion mismatch with the substrate
- those due to imposed loads during service

A list (Bennet, Rolls-Royce) of the Strains likely to be encountered under typical engine conditions are shown below.

Mechanism	Strain	Resistance Parameters	High Stress Zone
Thermal Gradients	0.2%	$\frac{\sigma_f \cdot k}{E \quad \alpha}$	Free surface
Expansion Mismatch	0.6%	$\frac{\sigma_f \cdot 1}{E \quad \alpha_c - \alpha_s}$	Substrate Interface
Applied Loads	0.5%	$\frac{\sigma_f \cdot E_s}{E_c}$	Substrate Interface

Where σ = failure strength, E = Youngs Modulus, k = Thermal Conductivity, α =expansion coefficient. Sub c and s refer to ceramic and substrate respectively.

In agreement with engine experience, the above shows that coating failures are more likely at the coating substrate interface and that thermal expansion mismatch dominates thermal gradients as the main stressing mechanism. This aspect will thus represent a major selection criterion.

Thermal Properties of Ceramics

The coefficient of thermal expansion for Inconel 713 is 13-14 10^{-6}/ °C (20°C to 530°C. In the development of thermal barrier coatings for 'conventional' gas turbine blades only a zirconia based system (with a of thermal expansion coefficient of 8 10^{-6}/ °C) has been successfully used in service. It is therefore very unlikely that ceramics with significantly lower thermal expansion coefficients will be viable candidates. Some materials with relatively low coefficients eg silicon nitride Si_3N_4 (3 10^{-6}/ °C), silicon carbide SiC (4.6 10^{-6}/ °C) and aluminium titanate Al_2TiO_5 =3 10^{-6}/ °C) are thus excluded.

Properties of oxides with relatively high coefficients of thermal expansion are listed in the table 1. These and other ceramics are discussed below.

Aluminium oxide (Al_2O_3)

Alumina has a relatively high expansion coefficient and the alpha phase is very stable up to 1700°C. It would also be expected to bond well with the oxide (alumina) scale formed on the turbine blade. However, in plasma sprayed coatings a meta-stable, gamma phase can predominant and care should be taken to check this aspect during processing.

Beryllium oxide (BeO)

There is little information on beryllia coatings and when processing, the presence of any free Be would represent a Health and Safety issue. This material would need further investigation.

Chromium Oxide ($Cr_2O_{3)}$

This is a commonly used ceramic applied extensively within the printing industry (mainly applied by Air Plasma Spraying). However, it has a relatively low coefficient of expansion at 5 10^{-6}/°C and has only moderate resistance to thermal shock.

Magnesium oxide (MgO)

The magnesia system appears to offer some very real advantages as a candidate ceramic for turbine blades. The expansion coefficient is 13.5 10^{-6}/°C. This material has been largely ignored in 'conventional' gas turbine developments due to it's unsuitability as a TBC (it has a thermal conductivity is 10-20 times that of zirconia!) However, in this application it could provide a very interesting, strain tolerant coating.

One potential problem may be in the bonding of MgO. Here it is worth considering an intermediate ceramic layer. One clear candidate is an alumina-magnesia spinel. This could be applied onto either a formed surface alumina scale (see bond coatings below) or onto a separate alumina coating.

Magnesia-Alumina-Silica System

This is a well established system and while the alumina-magnesia spinel mentioned above, other ceramics such as cordierite ($2Mg_2O.2Al_2O_3.5SiO_2$)
And mullite ($3Al_2O_3{\cdot}2SiO_2$) have relatively low coefficients of expansion.

Silicon Dioxide or Quartzite (SiO_2)

Of all the ceramics in the list, quartzite has a relatively low melting point with a maximum service temperature of only 1090 °C. This is perhaps too close to the actual operating temperature of the turbine.

Thorium Dioxide (ThO_2)

I have not found any information on the use of thoria as a coating. It is widely used to lower the work-function of tungsten in electrodes and it is also the most dense of the ceramics considered. However, availability and health and safety issues are likely to be problems.

Zirconium oxide, ZrO_2

As previously discussed, pure zirconia is not suitable for this application due to a phase change at about 800°C which can lead to cracking and coating failure. However, a stable, cubic phase can be produced for this temperature range by additions of a number of other oxides. The most successful composition is an

8wt%Y_2O_3 partially stabilised ZrO_2 with a thermal expansion coefficient of ~10. 10^{-6}/ °C.

Again, this is the only ceramic material currently applied to rotating parts of gas turbines and so, for this reason alone, should be included in the candidate coating list.

Bonding of ceramic coatings to nickel based alloys.

It is thought that the bonding of ceramic coatings to metals is by a largely mechanical mechanism and the use of bond coatings to provide a good 'key' and also provide a layer of intermediate thermal properties is generally highly beneficial.

Bond coats used for ceramic coatings on conventional turbine blades can include combinations of any of the following:

- a nickel aluminide layer deposited by CVD
- a platinum aluminide layer deposited by plating and then CVD
- an VPS/LPPS MCrAlY layer

However, while in conventional gas turbines these coatings provide corrosion resistance (not needed in this application) they also all act as alumina formers which appear to aid bonding.

The zirconia coatings applied to 'conventional' gas turbine blades are applied by the eb-PVD (see section 4) process. However, most coating failures occur at the ceramic/blade interface or more specifically at the metal oxide layer below the zirconia. Much work has been carried out to improve oxide scale adherence and hence bonding. Currently, the optimum solution appears to be a composite structure. First, a single-phase (Ni,Pt)Al coating is produced by electroplating Pt followed by a chemical vapour deposition (CVD) aluminising step. The outer surface is oxidised so that an alumina scale forms. This seems to be widely accepted as a premiere bond coating especially for higher-temperature eb-PVD TBC applications. The second stage is to deposit a thin alumina layer prior to applying the final zirconia coating.

(NB While Pt-aluminide coatings have been used for many years to protect turbine blades from corrosion/oxidation in 'conventional' gas turbines these conditions obviously don't apply to this project. It may be worth including a simple nickel aluminide as a more cost effective alternative.)

A second, alternative, bond coat can be provided by coating the blade (aluminised or not) with an MCrAlY layer using VPS/LPPS. Again, the eb-PVD coating is applied to a pre-oxidised (alumina) MCrAlY surface.

Based upon these developments it is likely that any alternative candidate ceramics will need to be treated in a similar way. However, as already mentioned, for MgO an alumina-magnesia spinel could also be used as an further, intermediate, bond layer.

Summary

Three main oxide ceramic systems appear to offer the best chance of success in providing durable coatings on HTGR turbine blades. These include partially stabilised zirconia, alumina and magnesia.

In order to enhance bonding, the blades should first be treated with a nickel aluminide or platinum aluminide layer followed by an eb-PVD alumina layer one of the main issues concerns the bonding of these ceramics to the nickel alloy turbine blade.

Prior to the final ceramic top-coat - In the case of magnesia, a further alumina-magnesia spinel layer could also be included as an aid to bonding.

Coating Technologies

There are probably only 3 main types of process that are currently used for coating turbine blades. These are discussed below.

Chemical Vapour Deposition (CVD)

As the name suggests, CVD is a chemical process which uses gas phase reactions to generate high vapour pressures of the species to be deposited. This is commonly either chromium or aluminium. The process is carried out at igh temperatures with the substrate held at typically 800°C - 1150°C. In the case of aluminium deposited onto a nickel based alloy the CVD process results in a thin (eg 10 micron) layer of nickel aluminide. Such coatings provide corrosion resistance.

However, such coatings are also used as bond coatings for TBC's. In this case, single-phase (Ni,Pt)Al coatings are produced by electroplating platinum followed by a CVD aluminising step. Such coatings appear to significantly improve the adhesion of eb-PVD TBC coatings. Although Pt-modified aluminide coatings have been in commercial service for over two decades, there is little understanding of the mechanism by which platinum improves oxide adherence.

While CVD aluminising is used for corrosion protection of 'conventional' gas turbine blades it will, as far as this project is concerned, be used solely to aid adhesion. However, since there is no corrosion problem in HTGR's then simple aluminising may be sufficient but both should be included in the test programme.

Electron Beam Physical Vapour Deposition (eb-PVD)

The PVD processes include evaporation, sputtering and ion plating but today, for gas turbine applications, the main process of interest is the high energy electron beam evaporator system or eb-PVD. Here high energy electron beams are used to melt alloy ingots and generate a vapour cloud into which the component is placed. A thin, smooth coating is built-up.

Eb-PVD is widely used in the gas turbine industry for applying MCrAlY metallic coatings on turbine blades and vanes for oxidation and corrosion protection. More recently, it has also been used to deposit zirconia thermal TBC's. The TBC's can be deposited onto an MCrAlY bond coat to aid adhesion and also provide corrosion resistance. The MCrAlY can be deposited by either eb-PVD or VPS/LPPS.

The main advantage of eb-PVD TBC's is their columnar structure which reduces the stress build-up within the body of the coating. These TBCs have superior degradation resistance than plasma sprayed versions. A further advantage is that the coatings have a very smooth surface finish.

Plasma spraying

There are two distinct types of plasma spraying. They are both based upon the same basic principals, but one is carried out in the open atmosphere and so is referred to as Air Plasma Spraying (APS) while the second is carried out in a vacuum chamber and so is referred to as Vacuum Plasma Spraying (VPS). In the USA VPS is often called Low Pressure Plasma Spraying (LPPS) but it is exactly the same as VPS.

Air Plasma Spraying (APS)

In all plasma spraying processes a plasma is produced using a dc arc. This is then forced through a nozzle to form a high temperature, high velocity plasma jet. The plasma forming gases are typically argon or nitrogen with additions of hydrogen. The coating material, in powder form, is injected into the jet where it is melted, accelerated and projected onto the component to form the coating.

In order to aid bonding the component surface is grit blasted prior to coating and cooling is often used to avoid oxidation. Coatings are applied in passes until the required thickness is achieved. Typical thickness is in the range 50-500 micron (2-20 thou). APS coatings are not fully dense and contain a number of defects. For most metal alloys the coatings have porosity levels of 2-10% and oxide levels ~3-5%. Bond strength is also limited. Similarly ceramic coatings contain pores and cracks and have significantly lower bond strengths. One way to alleviate this is to provide an intermediate metallic bond layer. This bond layer can also provide the substrate with additional corrosion resistance.

One of the main advantages of plasma spraying over other coating processes is the wide range of materials that can be deposited. In principal any material that has a stable liquid phase can be processed. Also as it is carried out in the open there is no limit on the size of component that can be processed. It is used extensively for coating gas turbine components using a wide range of materials.

Vacuum Plasma Spraying (VPS) or Low Pressure Plasma Spraying (LPPS)

The basic operation of VPS is the same as for APS except that the process is carried out in a vacuum chamber. A vacuum is used to remove oxygen and the chamber is then back-filled with argon to a pressure of about 100 mbar. These clean conditions allow the component to be pre-heated up to high temperature prior to coating without oxidation.

One of the main areas of use within the turbine industry is to apply MCrAlY type coatings (where M=Fe, Ni, Co) for corrosion protection. As with APS, the component is grit blasted prior to coating. It is then sputter cleaned and pre-heated to temperatures up to 1000°C. After coating the component is then subjected to a diffusion heat treatment to provide a strong bond with the component. It can then be shot peened and/or polished to achieve a smooth surface finish. Components have to be small enough to fit into the chamber (typically 1-2 m in diameter).

During repair of blades and vanes the old coating can be stripped by either diffusion/chemical means (eg Siemens Siclean process) or by high pressure water jet removal. Cleaned components can then be re-coated.

Another application for VPS is to provide the bond coat layer (again usually an MCrAlY) for thermal barrier coatings. The TBC's are not deposited by VPS as the coating density tends to be too high for a successful barrier coating. Instead a lower energy process Air Plasma Spraying (APS) is used (see above).

However, VPS can be used to spray ceramic coatings over a large range of compositions eg aluminium oxide, chromium oxide, zirconium oxide etc. However, in most cases these too would require a bond layer to even out the thermal mis-match between the base material and the ceramic. Now, since dense ceramic layers are potentially very beneficial as far as this project is concerned, the use of VPS/LPPS for depositing ceramics should perhaps be re-considered. Furthermore, although dense coatings are more highly stressed this project does not necessarily require thick coatings. Thus thin, VPS dense ceramics may provide an important processing route.

Coating Specifications and Test Procedures

In each process described above it will be necessary to produce well documented process data sheet. This will defined materials and the parameters used. It is also advisable to carry out some metallographical characterisation of the coatings so as to produce a well defined coating specification.

A second stage would be to define a test programme to optimise the coatings for their specific aplicatation eg a thermal cycling test to assess durability in the turbine environment.

Summary and Coating Matrix

The following matrix includes the candidate coatings and processes. (Note that coating thickness has not been included as a parameter.)

Number	Bond Coat	Process	Inter layer	Process	Top Coat	Process
1	(Pt,Ni)Al	CVD	Al2O3	eb-PVD	$Y_2O_3ZrO_2$	eb-PVD
2	(Pt,Ni)Al	CVD	Al2O3	eb-PVD	Al_2O_3	eb-PVD
3	NiAl	CVD	Al2O3	eb-PVD	Al_2O_3	eb-PVD
4	(Pt,Ni)Al	CVD	Al2O3	eb-PVD	MgO	eb-PVD
5	(Pt,Ni)Al	CVD	Al2O3 $MgO{\cdot}Al_2O_3$	eb-PVD	MgO	eb-PVD
6	(Pt,Ni)Al	CVD	Al2O3	eb-PVD	$MgO{\cdot}Al_2O_3$	eb-PVD
7	NiCrAlY	VPS	-	-	$Y_2O_3ZrO_2$	VPS
8	NiCrAlY	VPS	-	-	Al_2O_3	VPS
9	NiCrAlY	VPS	$MgO{\cdot}Al_2O_3$	VPS	MgO	VPS
10	NiCrAlY	VPS	-	-	$MgO{\cdot}Al_2O_3$	VPS

All the above coating processes are carried out at high temperature and so substrate materials should be relatively thick eg 5mm and made from the blade alloy.

Table 1 Properties of oxides with relatively high coefficients of thermal expansion (ASM data).

	Density	Melting	Point	Max Service	Temperature	Thermal Conductivity W/m · K			□	C	Hardness
Material	**g/cm³**	**°C**	**°F**	**°C**	**°F**	**At 100 °C (212 °F)**	**At 1000 °C (1830 °F)**	**At 1200 °C (2200 °F)**	**10^{-6}/°C**	**J/kg · °C**	**Mohs scale**
Alumina (Al_2O_3)	3.96	2050	3720	1950	3540	30	6	. . .	8	1050	9
Beryllia (BeO)	3	2550	4620	2400	4350	220	29	. . .	7.5	2180	9
Cordierite $Si_2Al_5.Mg_2O_{18}$						2.1			2.3	860	
Magnesia (MgO)	3.6	2850	5160	2400	4350	38	7	2.5	13.5	1170	6
Mullite ($3Al_2O_3 \cdot 2SiO_2$)	2.8	1850	3360	1800	3270	6	4	4	5	840	7.5-9
Quartzite (SiO_2)	2.65	1400	2550	1090	1990	. . .	. . .	2.1	8.6	1170	7
Sillimanite ($Al_2O_3 \cdot SiO_2$)	3.2	1800	3270	1800	3270	. . .	. . .	. . .	5	840	6.5
Spinel ($MgO \cdot Al_2O_3$)	3.6	2130	3870	1900	3450	15	6	. . .	8.5	1050	8
Thoria (ThO_2)	9.5-9.9	3220	5830	2700	4890	10	3	. . .	9.5	290	7
Zirconia (ZrO_2)	5.5-5.8	2700	4890	2400	3400	2	2.3	0.9	7.5	590	6.5

α Coefficient of linear thermal expansion from 25 to 800 °C (77 to 1470 °F)

C Specific Heat (mean) at 25 to 1000 °C (77 to 1830 °F)

TEST METHODOLOGIES

This section identifies appropriate methods for testing and assessing the effectiveness of the turbine blade coatings. The effectiveness of the coating is defined by the amount of silver that is allowed to diffuse through the coating into the underlying base metal. Therefore, a key step is quantifying the amount of silver in the base material. Chemical composition can be measured using a variety of techniques, including energy dispersive x-ray spectroscopy, Auger electron spectrometery, electron energy loss spectrometry, and Rutherford backscattering spectrometry, to name a few. Analytical techniques such as energy dispersive x-ray analysis or Auger electron spectrometry suffer from "peak overlap", in that the peaks of the emitted radiation (x-ray or Auger electrons) from two or more elements often overlap on the energy scale, making their concentrations difficult to quantify at high levels of precision. Of the available techniques, there are three that are appropriate for this application: Rutherford backscattering spectroscopy (RBS), neutron activation analysis (NAA), and electron microprobe analysis (EMPA), none of which require the handling of radioactive materials. The objective of this document is to describe each technique in detail, particularly as it may be applied to this project. A procedure for each analysis technique is also presented along with specimen preparation requirements. Finally, the strengths and weaknesses of all techniques are directly compared and summarized.

Analytical Techniques

In assessing the different analytical techniques, there are a number of important considerations that must be addressed. Foremost is the capability to measure low concentrations of silver in the base material. Following diffusion through the coating layer, Ag may be present in levels between a few ppb and a few atomic percent for effective or ineffective coatings, respectively. Further, sensitivity to Ag in pure Ni may be significantly different than the sensitivity in a commercial Inconel alloy.

The spatial resolution and ability to generate composition profiles as a function of distance from the coating/metal interface are also of interest. Some techniques can provide information on composition as a function of depth directly (EMPA) and others (NAA and RBS) require multiple steps of sample preparation and analysis.

The specimen preparation and geometry are also important factors. Each technique has different requirements in both the size of the sample and how the sample is prepared. For example, both NAA and RBS require that the protective layer be removed for accurate analysis. However, if a high level of Ag is measured in the underlying metal, the protective nature of the layer must certainly be questioned. If this layer has been removed, it is impossible to determine whether this failure is due to the properties of the layer (composition, structure, etc.) or defects in the structure created during deposition. Finally, availability of the analytical technique, time for

analysis, and ease of interpretation of data are also factors that must be considered. All these factors will be discussed for each technique.

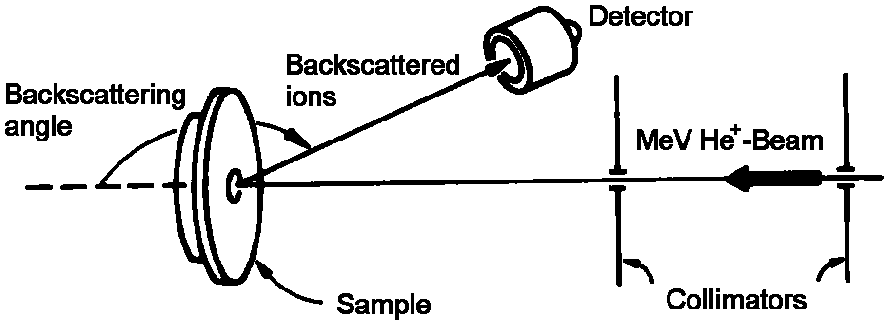

Figure 1: Schematic of Rutherford backscattering analysis.

Rutherford Backscattering Spectrometry

RBS involves measuring the number and energy of ions in a beam that backscatter off of atoms in the near-surface region of a sample at which the beam has been targeted. With this information, it is possible to determine atomic mass and elemental concentration versus depth below the surface. RBS is ideally suited for determining the concentration of trace elements heavier than the major constituents of the substrate. Its sensitivity for light masses, and for the makeup of samples well below the surface, is poor.

RBS is based on a simple physical phenomenon: the elastic collision between light, high energy particles and atoms of a target. This "collision" does not actually involve direct contact between the projectile ion and target atom. Energy exchange occurs because of Coulomb forces between nuclei in close proximity to each other. However, the interaction can be modeled accurately as an elastic collision using classical physics.

Monoenergetic light ions, for example 2 MeV He^{++} ions, impinge on a sample. A very small fraction of the ions will undergo near head-on collisions with the nucleus of a sample atom on or just below the surface. This scattering event is so rare that the attenuation of the beam intensity along its path in the target is insignificant and the effect is usually ignored. The backscattered particles will escape the sample and are collected, counted and energy-analyzed by a special detector. A schematic of the geometry of an RBS experiment is shown in Figure 1.

The energy measured for a particle undergoing a backscattering event at a given angle depends upon two processes: electronic energy loss and elastic energy loss. Particles lose energy while they pass through the sample, both before and after a collision. The amount of energy lost is dependent on the material's stopping power. A particle will also lose energy as the result of the collision itself. Finally, the intensity of backscattered particles reflects the concentration of target atoms. As such, a single RBS spectrum contains information about the masses of the target elements, their concentrations, and the concentration depth profiles. From an analytical point of view, RBS is most sensitive to heavy mass elements in the form of thin films on low mass substrates. Thin films of high mass elements give high intensity RBS signals free of background. RBS measurements of lighter elements are more difficult due to the low signal-to-background ratio.

RBS analysis is commonly performed with 2 MeV He^{++} ions, using an accelerator such as the Tandetron ion accelerator in the Michigan Ion Beam Laboratory for Surface Modification and Analysis at the University of Michigan. The range of 2 MeV ions in Ni is ~ 3.5 μm, however, the effective range and depth resolution for RBS is significantly less than the He range as particles must scatter and leave the target in order to be detected. The practical range for RBS analysis with 2 MeV He^{++}ions is approximately 380 nm. The depth resolution depends on the target, but for 2 MeV He^{++} into Ni, the depth resolution is ~ 30 nm. This resolution may be further improved by using glancing angle techniques. Spatial resolution is limited to the size of beam, typically down to 2 mm. Some higher resolution systems offer spatial resolution down to 0.5 mm. The sensitivity is determined by the amount of the element that must be present to yield a statistically significant number of counts above background in a practical analysis time (approximately 30 minutes). For high Z species, such as Ag, elemental sensitivity is typically between 0.01 and 0.001 at% (10-100 appm). Therefore, RBS is a suitable technique for the examination of Ag diffusion in Ni or Ni-base alloys. The sensitivity for light, low Z, elements is considerably less.

Since RBS reactions can be calculated from first principles, numerous codes are available to perform one of two operations: 1) to simulate the RBS experiment given the experimental parameters (angles, masses, detector efficiency), or 2) given the experimentally determined RBS spectrum and the experimental parameters, determine the composition vs depth profile (reverse approach). Examples of codes of each type are RUMP [1] and SIMNRA [2] for the forward codes and IBA [3] for the reverse codes. The forward codes are most useful when studying a relatively unknown system. The reverse approach works best when the sample composition is known, and an exact determination of the composition vs. depth profile is needed.

The RUMP code [1] was used to perform several simulations of the measurement of Ag in a Ni specimen. All simulations used 2 MeV He^{++}incident on a Ni specimen with a backscattering angle of 170°. The RBS spectrum of pure Ni is illustrated in Figure 2. The leading edge for the Ni peak occurs at an energy of 1.51 MeV. The RBS spectrum for Ni with a thin, 5 nm layer of Ag is shown in Fig. 3. Note that the heavy Ag layer causes the backscattering of He at higher energies than does the underlying Ni. Figure 4 illustrates the RBS spectrum from a sample with a small, uniform amount of Ag (20 appm) uniformly distributed. The Ni-edge from Figure 2 is unchanged, and the Ag appears as a plateau extending beyond the Ni peak at a very low magnitude rather than the sharp peak resulting from a surface layer, as shown in Figure 3. Comparison of the spectra in Figures 2 and 4 illustrates that RBS is capable of detecting Ag in Ni down to at least 20 appm, although this is close to the minimum amount detectable.

As a result of diffusion, the actual Ag concentration will not be uniformly distributed. Rather, following heat treatment, any Ag that permeates the oxide barrier will diffuse into the underlying metal, which also influences the RBS spectrum. The RUMP program also provides simulations of RBS spectra for a variety of composition profiles. A Ag diffusion profile is simulated using the error function [4] with a diffusion coefficient of $2x10^{-10}$ cm^2/s [5]. The simulated RBS spectrum for Ag diffusing into a Ni specimen is illustrated in Figure 5. In this case, the Ag peak tails off at a greater specimen thickness (corresponding to lower energies). This is consistent with reduced Ag concentrations at the greater specimen depths as well. This

also shows that concentration profiles may be determined from measured spectrum if simulations are carefully applied. However, concentration profiles can only be determined for thickness up to ~400 nm. For concentration profiles beyond this range, successive layers of material must be removed followed by additional RBS analysis. Thus, beyond the first 400 nm, depth resolution using successive layer removal is dependent on the thickness of the layers removed and accurate removal of layers less than ~1 μm becomes very difficult.

While RBS is capable of better than 20 appm sensitivity of Ag in pure Ni, it must be noted that in a commercial alloy, the resolution drops dramatically due to the inclusion of elements of mass similar to that of Ag. RUMP was used again to simulate the RBS spectrum for 2 MeV He^{++}into Inconel 718 with 20 appm Ag following a diffusion profile. The resulting spectrum is illustrated in Figure 5. The distinct Ag plateau shown in Figure 4 disappears when other elements are added to the pure Ni base. As a result, the sensitivity of Ag diffused into Inconel 718 is only ~ 0.1 at%.

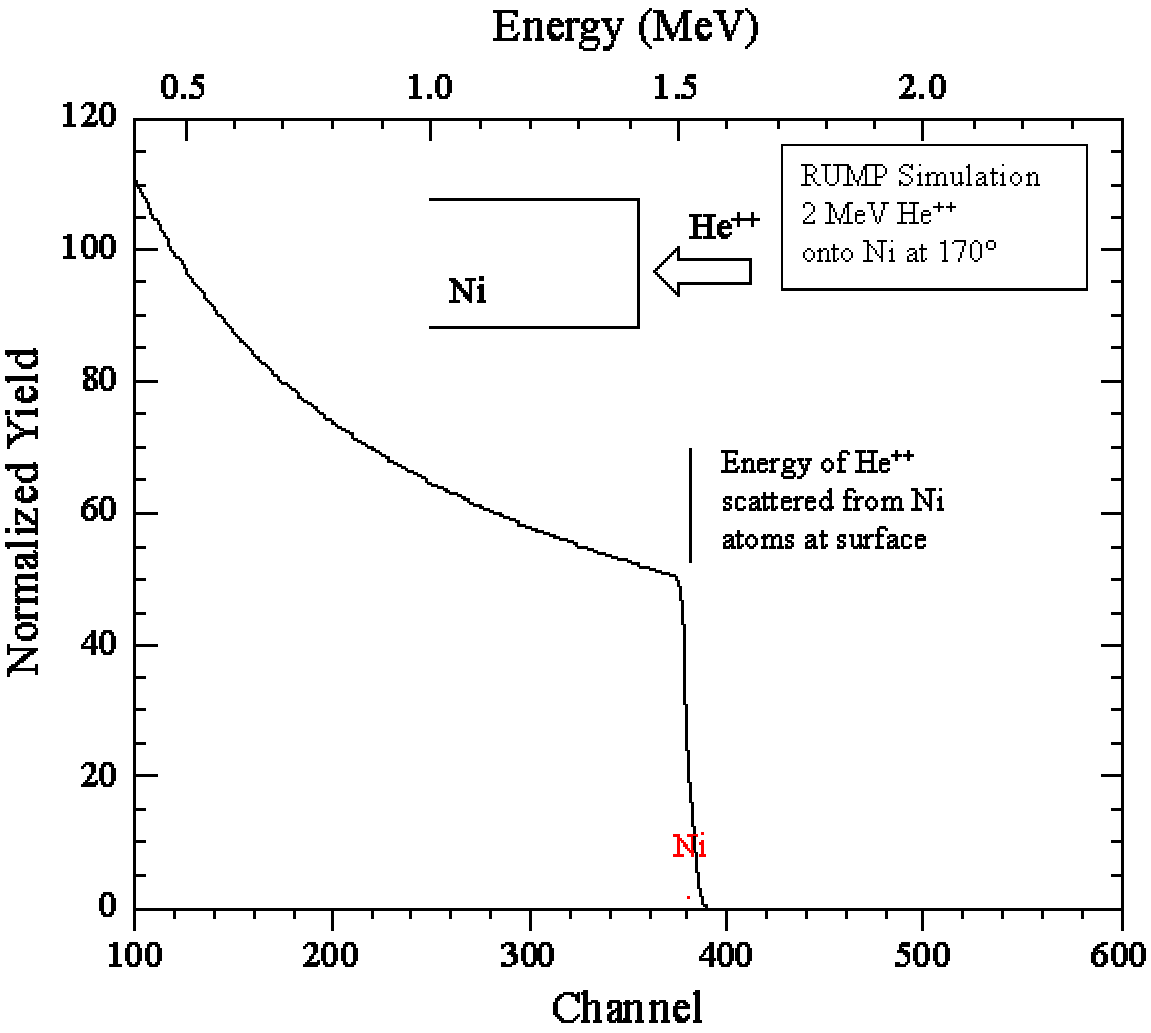

Figure 2: Simulated RBS spectrum for 2 MeV He^{++} on pure Ni.

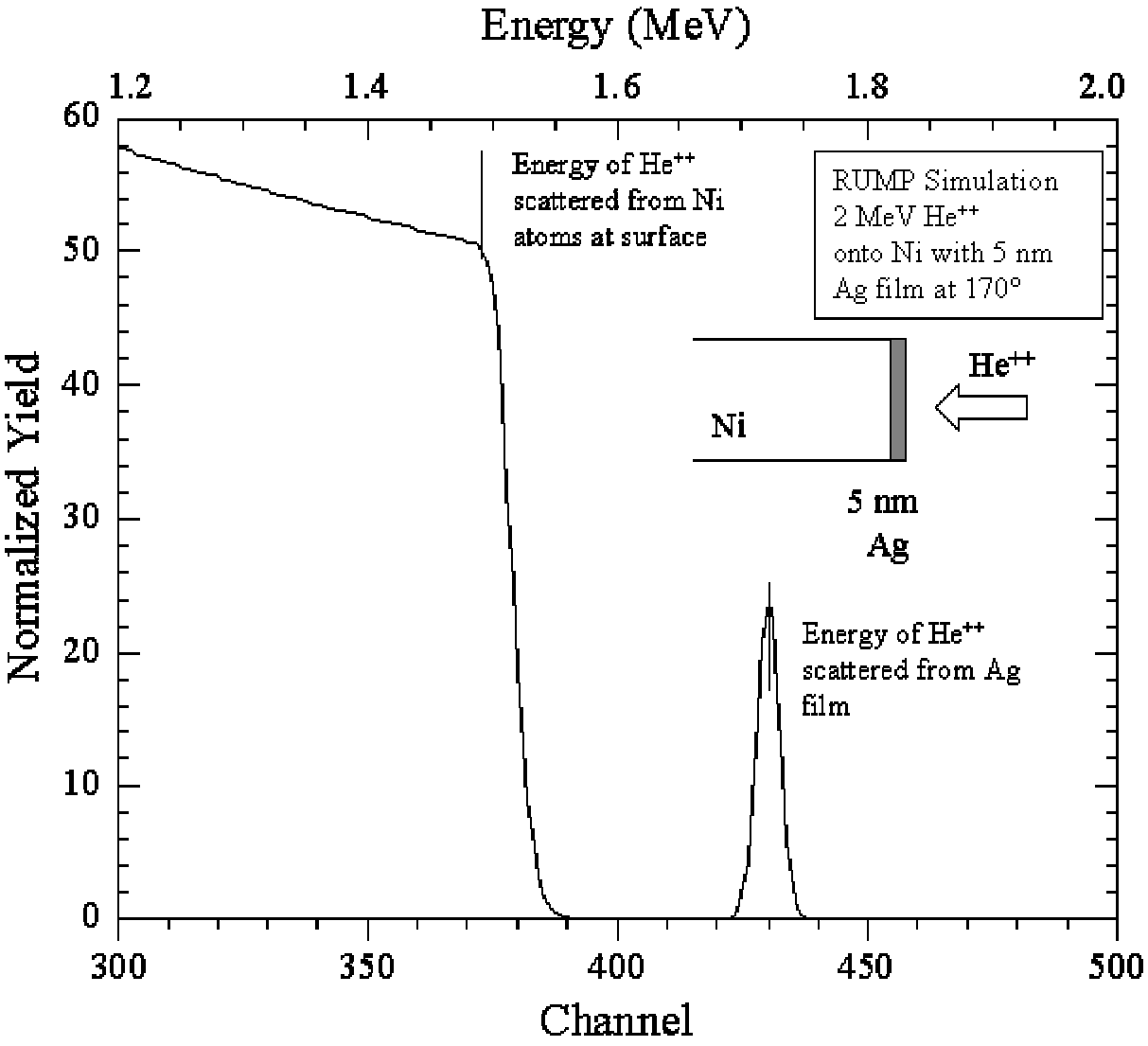

Figure 3: Simulated RBS spectrum for Ni with a 5 nm layer of Ag on the surface.

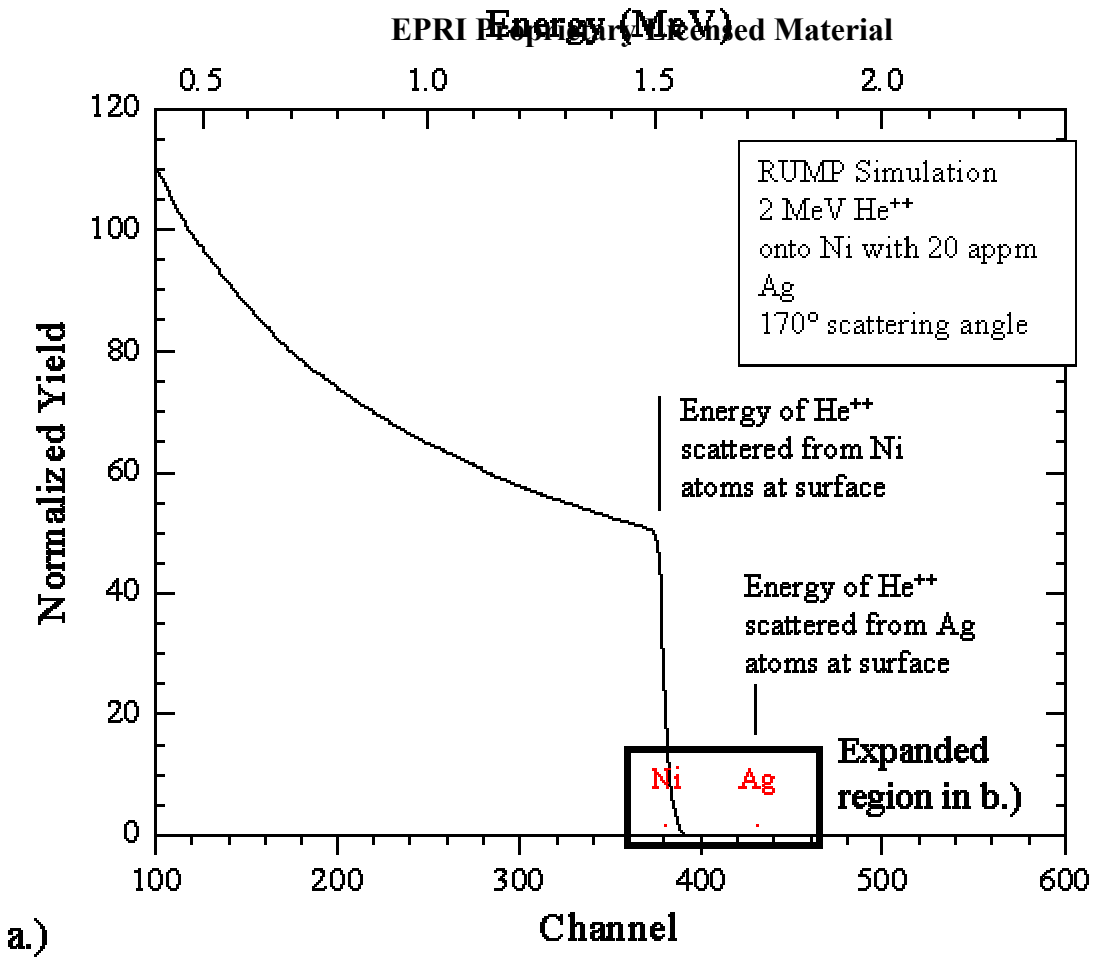

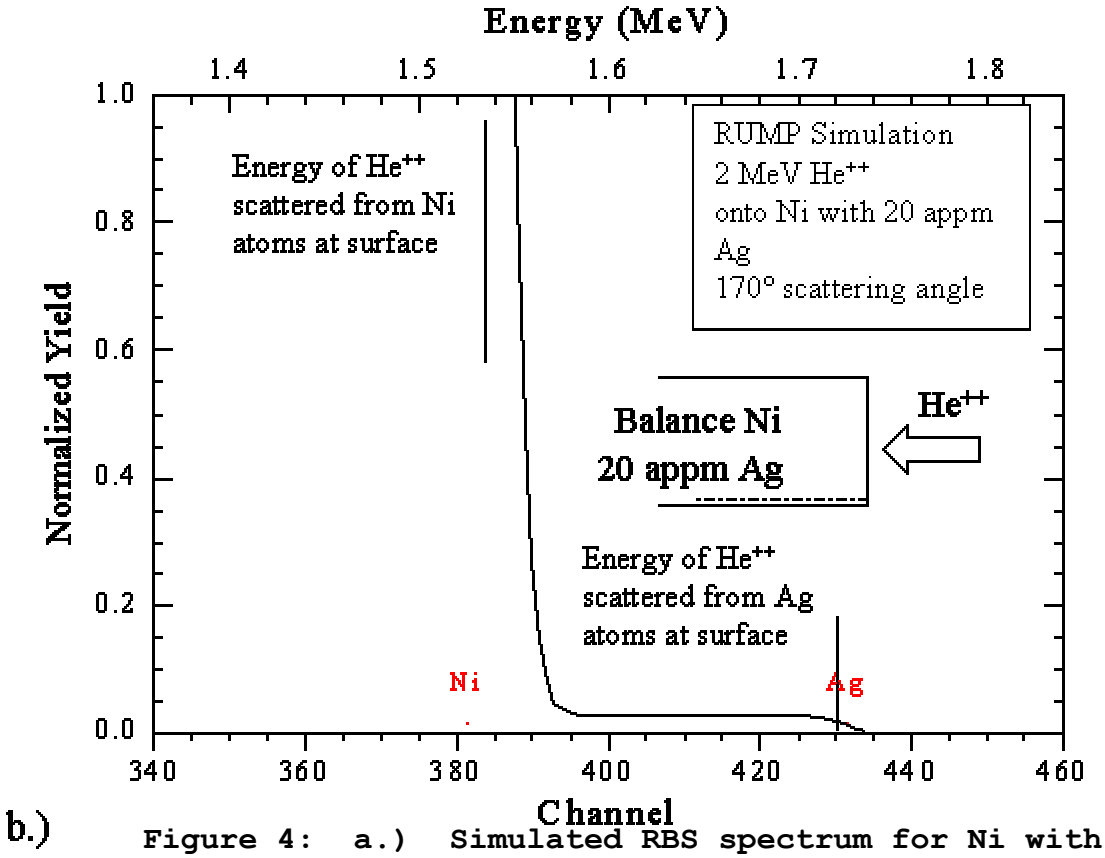

Figure 4: a.) Simulated RBS spectrum for Ni with 20 appm Ag distributed uniformly through the specimen. b.) Expanded view of Ag plateau.

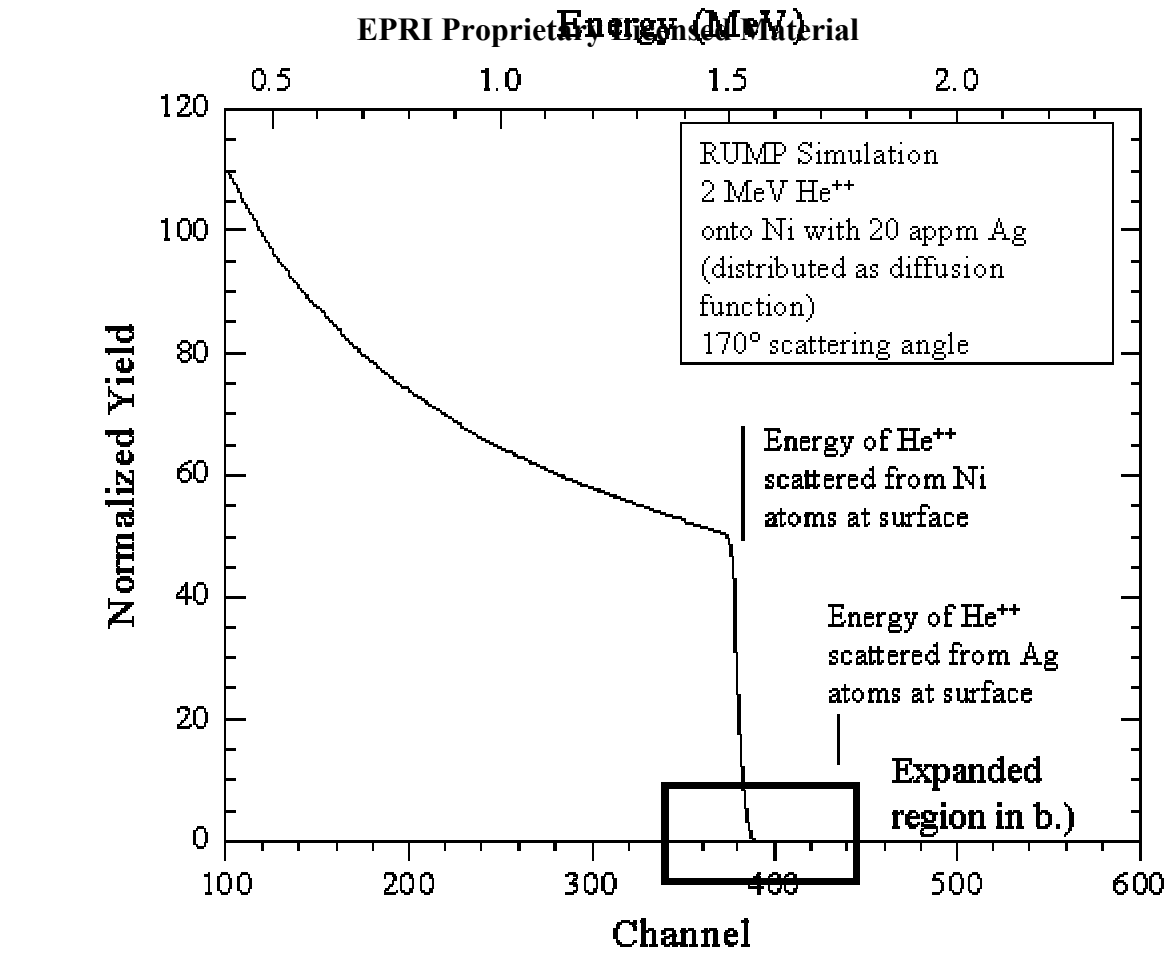

a.)

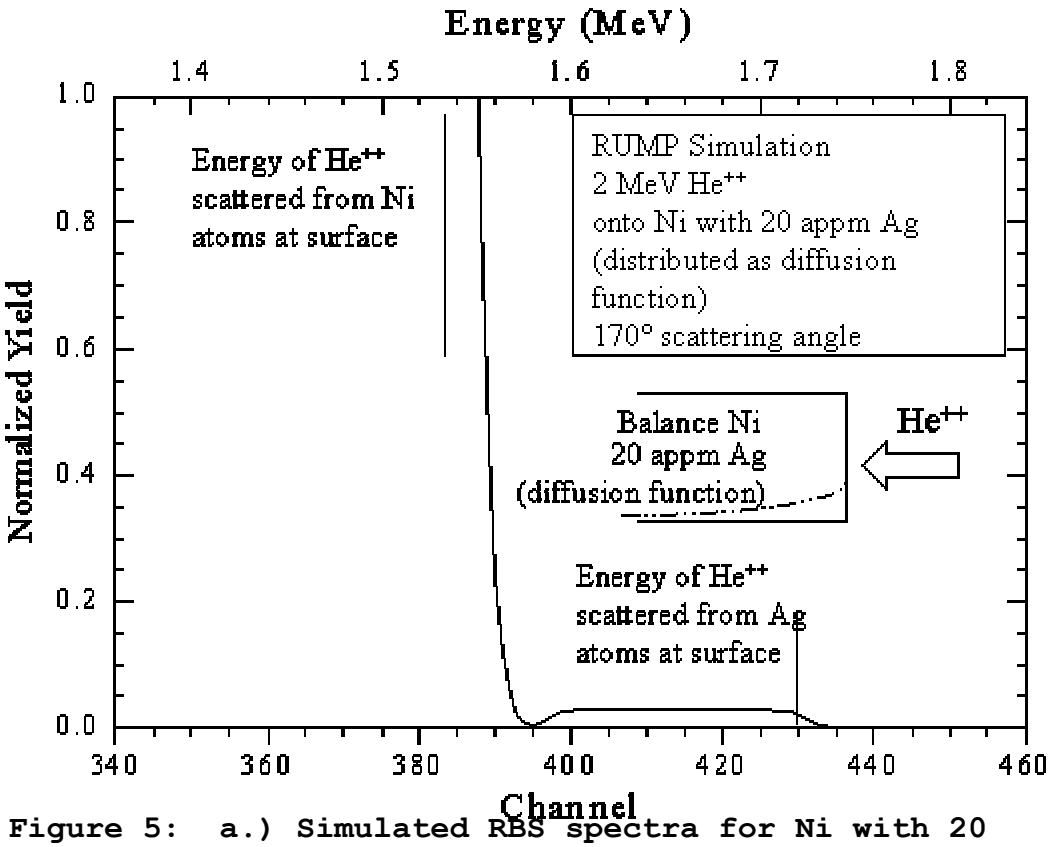

b.)

Figure 5: a.) Simulated RBS spectra for Ni with 20 appm Ag following a diffusion profile. b.) Expanded view of Ag plateau.

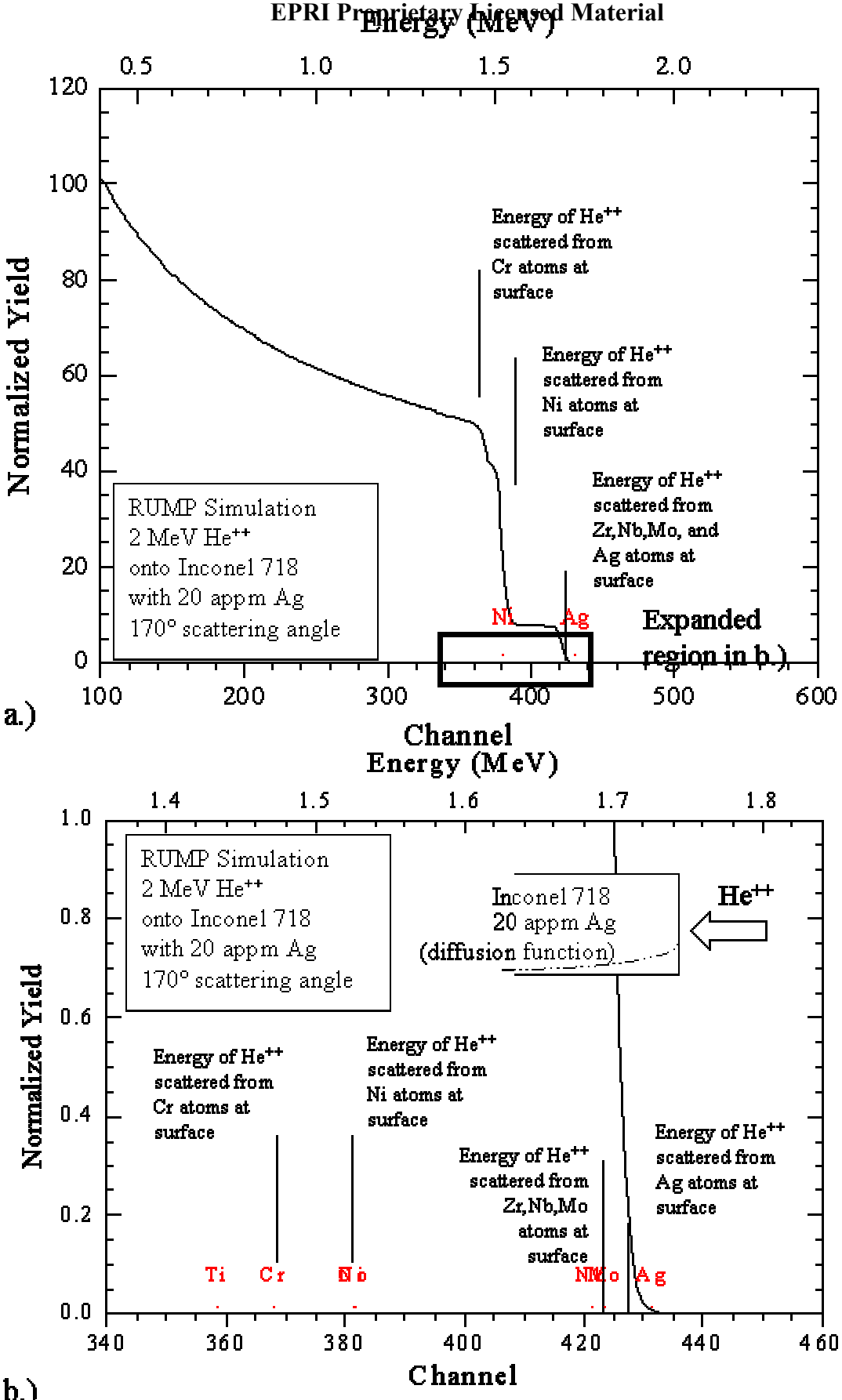

Figure 6: a.) Simulated RBS spectra for Inconel 718 with 20 appm Ag following a diffusion profile. b.) Expanded view of Ag plateau

RBS Procedure

Following heat treatment to diffuse Ag through the protective layer, the sample must be prepared for RBS analysis by removing the oxide layer without altering the underlying alloy. The sample is then loaded into the target chamber and the chamber is pumped down to a high vacuum (~10^{-6} torr) prior to analysis and the predefined scattering angle is verified. A He^{++} beam is then created and focused onto the sample. Beam currents of 20-50 nA are typical. An EG&G-Ortec detector is used to measure the backscattered particle energy and the resulting spectrum is collected using a multi-channel analyzer and MAESTRO analysis software. The total amount of He^{++} beam is measured simultaneously using an EG&G current integrator. Typical spectrum acquisition takes approximately 20 minutes, and following acquisition, the spectrum is analyzed (for sample composition, film thickness, etc) offline using the RUMP analytical program. Depending on the complexity of the spectrum, analysis takes between 0.5 and 2 hours.

This procedure is typical of analysis performed at the Michigan Ion Beam Laboratory at the University of Michigan. This work can be performed at other university and government facilities such as Cornell University, Texas A&M University, and Sandia National Laboratory. This type of service is also provided at firms such as Accurel Systems International and Evans Analytical Group.

Summary of RBS Analysis of Ag in Ni

Advantages:

- High sensitivity for Ag in Ni (~ 20 appm)
- No residual radioactivity
- Analysis can be performed in approximately 30 min. to 1 hour
- Depth profiles can be determined using simulation programs to depths of about 400 nm with a depth resolution of about 30 nm.

Disadvantages:

- Technique is destructive
- Protective oxide must be completely removed for analysis
- Sensitivity of Ag in commercial Inconel 718 is limited (~0.1 at%)
- Depth profiles beyond 400 nm cannot be measured directly unless successive layers of material are removed. Resolution using successive layer removal is dependent on the thickness of the layers removed, ~1 micron.

Neutron Activation Analysis

Neutron activation analysis (NAA) is a sensitive analytical technique useful for performing both qualitative and quantitative multi-element analysis of major, minor, and trace elements in a wide variety of samples. In general, NAA is a non-destructive analytical technique where the sample or artifact may be returned to the researcher after analysis. For many elements and applications, NAA is capable of sensitivities on the order of parts per million or better.

The principle involved in neutron activation analysis consists of first irradiating a sample with neutrons in a nuclear reactor to produce specific radionuclides. After irradiation, the characteristic gamma rays emitted by the decaying radionuclides are quantitatively measured by gamma spectroscopy, where the gamma rays detected at a particular energy are characteristic of a specific radionuclide's presence. The gamma ray spectrum is then analyzed to determine the concentrations of the various elements in the sample. With neutron activation analysis it is possible to measure quantitatively up to approximately 60 different elements in small samples. The lower limit of detection is on the order of parts per million to parts per billion depending on the element analyzed and the activity of the bulk sample matrix.

The most common nuclear reaction used for NAA is the neutron capture or (n,γ) reaction. This reaction is illustrated in Figure 7. When a neutron interacts with the target nucleus, a compound nucleus forms in an excited state. The compound nucleus will almost instantaneously decay into a more stable configuration through emission of one or more prompt gamma rays, which are characteristic of the decaying species. This decay often yields a radioactive nucleus, which also decays by emission of one or more characteristic, delayed gamma rays, but at a much slower rate according to the unique half-life of the radioactive nucleus.

NAA can be performed using any of several types of neutron sources (reactors, accelerators,

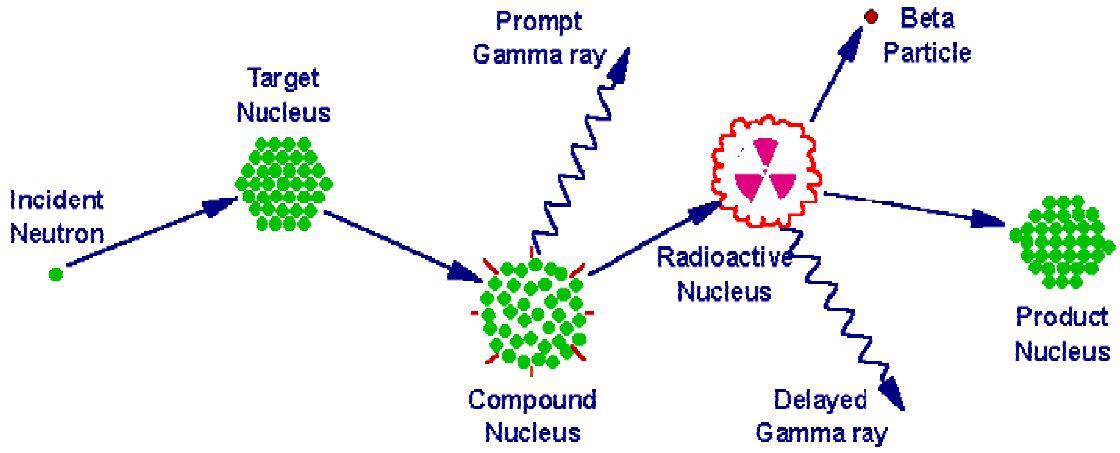

Figure 7: Diagram illustrating the process of neutron capture by a target nucleus followed by the emission of gamma rays [6]

and radioisotopic neutron emitters). Nuclear reactors are the preferred neutron source as they

provide the highest neutron fluxes and the most flexibility in terms of neutron spectrum. Neutron energy plays a large role in determining the nature of nuclear reactions that are possible. Interactions with thermal neutrons result in the (n,γ) reaction described above and are heavily utilized in NAA analysis. Fast neutrons (energies above 0.5 MeV) contribute very little to the (n,γ) reaction, but instead induce nuclear reactions where the ejection of one or more nuclear particles - (n,p), (n,n'), and (n,2n) - are dominant. By tailoring the location of samples within the reactor during irradiation (and hence, the neutron energy spectrum) specific reactions can be promoted or suppressed. Typically, samples are irradiated for times varying between a few seconds to a few hours to activate the specimen.

Following irradiation, the activity of the sample is then characterized. The instrumentation used to measure gamma rays from radioactive samples generally consists of a semiconductor detector, associated electronics, and a computer-based, multi-channel analyzer (MCA/computer). Most NAA labs use intrinsic germanium (HPGe) detectors that operate at liquid nitrogen temperatures (77 K) by mounting the germanium crystal in a vacuum cryostat. The most common type of detector is the coaxial detector, which is useful for measurement of gamma rays with energies in the range 60 keV to 3.0 MeV. For most NAA applications, a detector with 1.0-keV resolution or below at 122 keV and 1.8 keV or below at 1332 keV is sufficient. A sample spectrum is illustrated in Figure 8. Intensities for each peak of interest can be determined and used to calculate elemental concentrations.

The sensitivities for NAA depend on the irradiation parameters (i.e., neutron flux, irradiation and decay times), measurement conditions (i.e., measurement time, detector efficiency), and nuclear parameters of the elements being measured (i.e., isotope abundance, neutron cross-section, half-life, and gamma-ray abundance). All these factors combined must yield an activity that is greater than the background activity to measure the composition of any given element. The accuracy of an individual NAA determination usually ranges between 1 to 10 percent of the reported value. Table 2 lists the approximate sensitivities for determination of elements assuming interference free spectra and a neutron flux of ~ 1 x 10^{13}/cm^2/s (typical of the Ford Nuclear Reactor at the University of Michigan). The sensitivity listed is in picograms of activated element, which is the minimum weight of the element that must be present in the sample to be detected accurately. That is, to detect Ag for example, a minimum of 1 ng must be present to be activated to statistically significant levels. Thus, to detect Ag in Ni at a level of 1 wppm (0.5 appm), a 1 mg sample of Ni is needed. To detect Ag in Ni at levels of 1 wppb (0.5 appb), a 1 g sample must be activated.

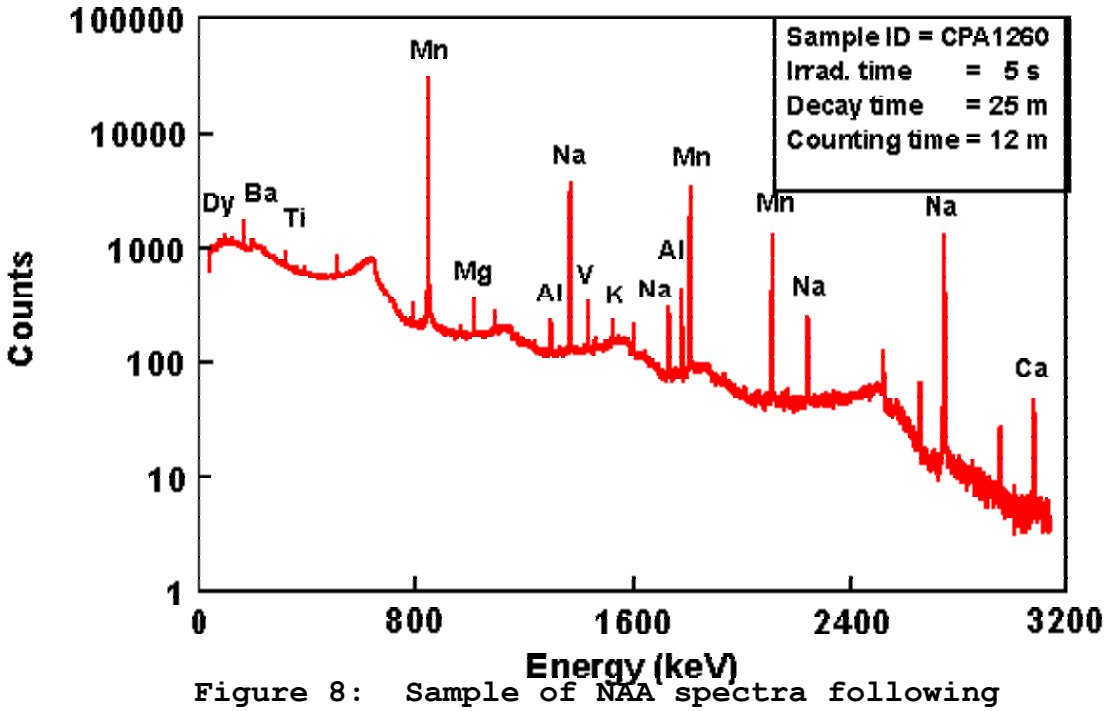

Figure 8: Sample of NAA spectra following activation.[6].

Table 2. Estimated detection limits for NAA using decay gamma rays[6]. Assuming irradiation in a reactor neutron flux of $1x10^{13}$ n cm^{-2} s^{-1}.

Sensitivity (picograms)	Elements
1	Dy, Eu
1 - 10	In, Lu, Mn
10 - 100	Au, Ho, Ir, Re, Sm, W
100 - 1E3	Ag, Ar, As, Br, Cl, Co, Cs, Cu, Er, Ga, Hf, I, La, Sb, Sc, Se, Ta, Tb, Th, Tm, U, V, Yb
1E3 - 1E4	Al, Ba, Cd, Ce, Cr, Hg, Kr, Gd, Ge, Mo, Na, Nd, Ni, Os, Pd, Rb, Rh, Ru, Sr, Te, Zn, Zr
1E4 - 1E5	Bi, Ca, K, Mg, P, Pt, Si, Sn, Ti, Tl, Xe, Y
1E5 - 1E6	F, Fe, Nb, Ne
1E7	Pb, S

As illustrated in Table 2, NAA is certainly capable of analyzing samples with low levels of Ag following heat treatments to cause diffusion through the protective layer. However, several complications must be addressed. First, in order for this to be a useful technique, the oxide layer must be removed from the sample without disturbing the underlying metal. Exposure to the neutron flux will activate the silver, regardless of where it is located. Therefore, only the metal sample should be activated. Another complication is that the measurement yields the total amount of Ag in the sample, without regard to how it is distributed. Removing successive layers of material and then performing spectroscopy after each layer removal is the only way to obtain composition profiles. The depth resolution is then dependent on the accuracy of the removed layer thickness, or about 1-10 μm.

The activation of a 10-g Ni specimen containing 1 wppm Ag (0.5 appm Ag) was simulated using an online activation calculator [7]. The simulation was performed using a mixed (thermal and fast) neutron spectrum at a flux of 1 x 10^{13} n/cm^2/s for 15 minutes, followed by a 15-minute waiting period before counting. Table 3 summarizes the results of this analysis. The weights listed in the first column indicate the amount of each specific isotope listed in the second column (that is, 10 μg of naturally occurring Ag contains approximately 4.9 μg of Ag-107 and 4.6 μg of Ag-109). The possible activation reactions and resulting daughter products are listed for each isotope Ag in the third and fourth columns. The final two columns list the total activity at the time of the measurement (after 15 minutes of irradiation and a 15 minute waiting period) and the half-life the each active daughter product. After the 15-minute waiting period, the silver isotopes accounted for 250 kBq of activity, which is ample for accurate analysis at the appm level. However, it is also important to note that the isotopes resulting from activation of Ni have half-lives on the order of many years, rendering the sample radioactive following analysis.

NAA can also be performed using Inconel 718 samples. Clearly, the additional elements of the commercial alloy will also be activated during irradiation. This has a considerable impact on the total activity and the complexity of the spectrum as the capture cross section for Mo, Ti, Al, and Cb is quite high resulting in activities over 3 orders of magnitude greater than those from Ni. Despite this, there is no reduction in the amount of activity from Ag and no loss of resolution for Ag in Inconel in comparison to Ag in pure Ni as the isotopes created from Ag are unique.

Table 3: Summary of activity from silver following simulated neutron activation of a 10 g Ni sample doped with 1 wppm Ag (0.5 appm) (1 x 10^{13} n/cm^2/s, fast and thermal spectrum) irradiated for 1 hour, followed by a 15 minute waiting period before counting)

Parent Nucleus Mass	Isotope	Reaction	Isotope	Activity	Half-life
Silver (10.00 μg) (1 wppm)					
4.9 μg	Ag-107	(n,G)	Ag-108	256.9 kBq	2.370 m
	Ag-107	(n,p)	Pd-107		6.500e6 a
4.6 μg	Ag-109	(n,G)	Ag-110	436.8 μBq	24.57 s
	Ag-109	(n,2n)	Ag-108		2.370 m
	Ag-109	(n,p)	Pd-109		13.45 h
			Ag-109m		39.61 s
	Ag-109	(n,t)	Pd-107		6.500e6 a

NAA Procedure

Following heat treatment to diffuse Ag through the protective layer and sample preparation to remove the oxide layer, the sample is placed inside the reactor core using a pneumatic transfer tube system. The sample is irradiated within the reactor core for approximately 1 hour at a flux of ~1 x 10^{13} n/cm^2/s. Following irradiation, the sample is transferred directly to the counting

laboratory, again using the pneumatic transfer system. Prior to counting, the sample is allowed to cool for up to 15 minutes to reduce the amount of background activity. The sample is then counted using a HP intrinsic Ge detector and the energy spectrum is acquired using a multi-channel analyzer. The sample is counted for approximately 10 minutes, providing enough counts under the Ag peak for suitable statistics. Following counting, the spectrum is analyzed and the Ag concentration is calculated. In total, NAA requires approximately 2 hours for a complete analysis.

NAA can be performed at numerous locations, most being universities with research reactors. NAA is routinely performed at the Ford Nuclear Reactor in the Phoenix Memorial Laboratory at the University of Michigan. In addition to the University of Michigan, Texas A&M University, Kansas State University, North Carolina State University all perform NAA. This analysis can also be performed at Oak Ridge National Laboratory and the National Institute of Standards and Technology have this capability.

Summary of NAA Analysis of Ag in Ni

Advantages:

- High sensitivity for Ag in Ni (~ 0.5 appm)
- Analysis can be performed in approximately 1 to 2 hours
- Sensitivity for Ag in commercial Inconel 718 is still quite high (0.5 appm)

Disadvantages:

- Technique is destructive of sample
- Protective oxide must be removed for analysis
- Sample becomes mildly radioactive
- Depth profiles cannot be measured directly unless successive layers of material are removed. Depth resolution is governed by the control of thickness of removed layers, typically 1 μm.

Electron Microprobe Analysis

Electron microprobe analysis (EMPA) is a third technique that is useful for determining chemical composition. Electron microprobe analysis is used for rapid analysis of samples at a spatial resolution of about 1-3 μm. The layout of a modern microprobe is essentially similar to that of an SEM. Some instruments are hybrid microprobes/SEMS. A microprobe consists of an electron gun, a probe-forming system, and imaging system, and an X-ray detection system, shown schematically in Figure 9.

Most EMPA systems use an electron gun that operates between 1 and 50 kV. The electron gun operates typically at voltages up to 50 kV, which directly influences many factors, as will be discussed below. Small probes between 200 nm and 1 μm in size on the sample with currents between 1 and 100 nA, respectively, are possible with most standard systems currently available. Microprobes, with few exceptions, use wavelength dispersive X-ray spectroscopy (WDX) spectrometers because of their superior resolution when compared to more common energy dispersive spectrometers, and the ability to detect elements as light as Be. However, WDX detectors can only accept a single wavelength X-ray at any given time, creating the need for multiple detectors on a single instrument (up to 6 is typical).

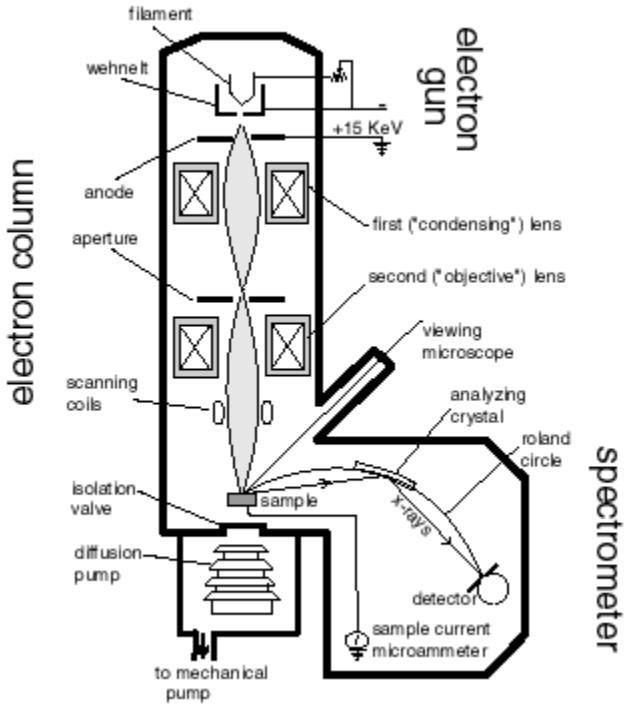

Figure 9: Schematic of EMPA system.[8]

Electron bombardment of a sample produces a large number of effects from the target material (Figure 10). These effects include: X-rays (both continuum and characteristic) backscattered and transmitted electrons, secondary electrons, Auger electrons, cathodoluminescence, and heat. Of particular interest for elemental analysis is X-ray emission. If the energy of the incident electron is high enough to eject inner shell electrons, then characteristic energy loss electrons will be generated and characteristic X-rays will be emitted from the ionized atom as an outer shell electron falls into the inner shell vacancy. This is illustrated schematically in Figure 11. Clearly, larger number of electron energy levels leads to a larger number of different characteristic x-rays, which can be generated. It is also important to note that if the incident beam energy is insufficient to knock the inner shell electron from its shell, no characteristic x-ray will be generated. The yield of x-rays produced by an energetic incident electron rises sharply when the energy of the incident electron is greater than the binding energy. Therefore, care must be taken to ensure that the operating voltage is sufficient to excite the element of interest. For Ag, the K□

and K□ energies are 22.1 and 24.9 keV, respectively. Thus, an operating voltage of 30 kV is necessary to measure Ag.

An important property of a WDX spectrometer is that it acts as a monochromator, focusing the individual wavelength X-rays onto the detector. The elemental resolution of the spectrometer is controlled by the perfection of the spectometer crystal, which, in turn, influences the range of wavelengths, which are focused into the detector. In general, most EMPA systems have an elemental resolution on the order of a few hundred ppm. The resolution of most EMPA systems is 400 ppm (0.04 wt%) for both Ni and Ag.

The excited volume of material (and hence, spatial resolution) is also of great interest. The

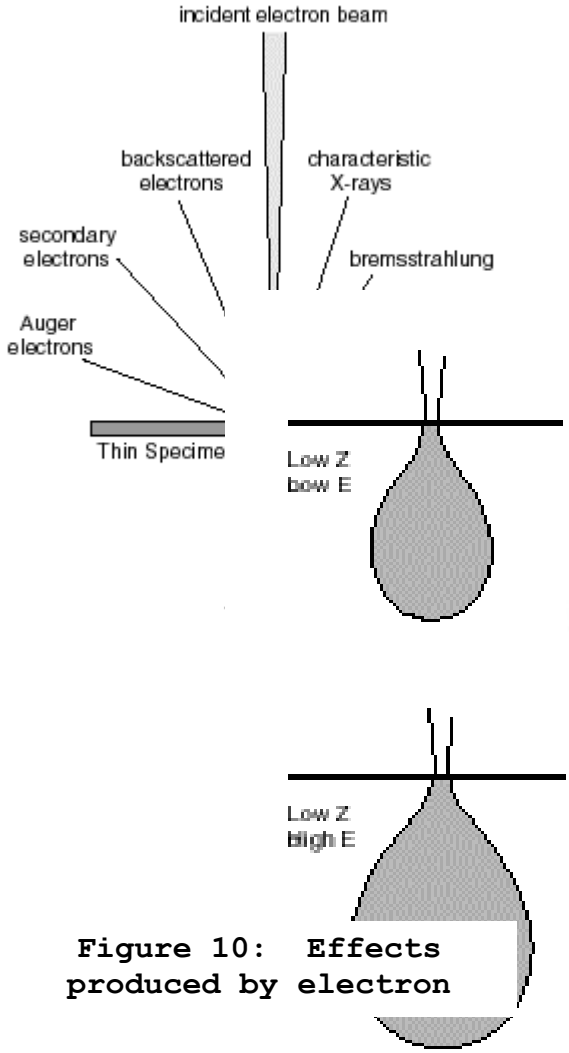

Figure 10: Effects produced by electron

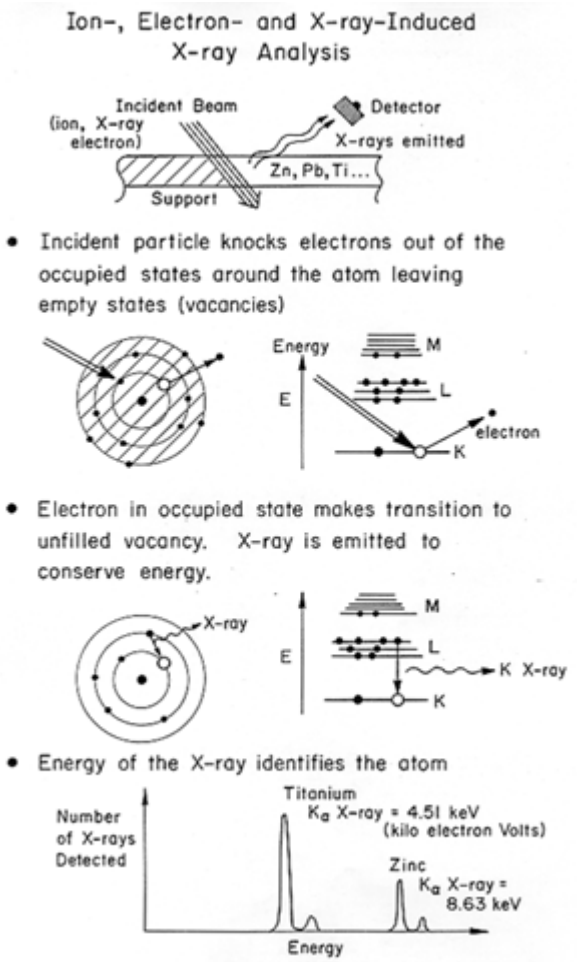

Figure 11: Schematic illustration of characteristic x-ray

Figure 12: Illustration of sample volume excited by incident electron

excitation volume is a hemispherical or a jug-shaped region with the neck of jug at the specimen surface, as illustrated in Figure 12. The depth of penetration of an electron beam and the volume

of sample with which it interacts are a function of its angle of incidence, the magnitude of its current, the accelerating voltage, and the average atomic number (Z) of the sample. Of these, accelerating voltage and sample density play the largest roles in determining the depth of electron interaction. Electron penetration generally ranges from 1-5 μm with the incident beam in a direction perpendicular to the sample. For a 30 keV beam incident upon Ni, the penetration depth is approximately 2 μm.

A final consideration is the specimen geometry required for EMPA analysis. For the highest elemental resolution, EMPA requires optically flat, stable specimens. Specimen size is limited by the size of the detector chamber but samples up to several cm in length and several cm in depth can typically be accommodated. The small spatial resolution of the incident probe does allow for easy compositional profiling. The composition of Ag could be determined as a function of depth through the protective oxide layer, the oxide-metal interface, and the underlying Ni (or Inconel) substrate without any loss of elemental resolution if the analysis is performed on a cross-section of the sample.

EMPA Procedure

EMPA analysis is fairly straightforward. Following heat treatment to diffuse Ag through the protective layer and cross-sectional specimen preparation, the sample is placed in the vacuum chamber of the EMPA system. The University of Michigan uses a Cameca SX-100 Electron Microprobe Analyzer. The Cameca uses a tungsten filament and operates at 30 kV for analysis of Ag (although voltages up to 50 kV are possible). After reaching appropriate vacuum (~10^{-6} torr), the sample is placed into the electron column and the area to be analyzed is located. EMPA takes approximately 30 minutes for each specimen.

EMPA analysis can be performed at many other locations, including most universities (Stanford, the University of Washington, and Texas A&M are just a few) and national laboratories. Commercial companies such as Accurel and Evans Analytical Group also provide these services.

Summary of EMPA Analysis of Ag in Ni

Advantages:

- No residual radioactivity
- Analysis can be performed in approximately 30 minutes
- Depth profiles can be measured directly
- High depth resolution (~1-2 μm)

Disadvantages:

- The technique is destructive

- Relatively poor sensitivity for Ag in Ni (~ 400 appm)
- Requires cross-sectional sample.

Sample Geometries and preparation for analysis of Ag in Ni

Each of the three analytical techniques described above require some specimen preparation between heat treatment and analysis. In this section, the different specimen geometries and preparation techniques are described. The advantages and disadvantages associated with each technique are also listed.

Plan view

Both NAA and RBS analyses are conducted in plan view. RBS can be used to determine depth concentration profiles from the collected spectra to a depth of about 400 nm, after which, successive layer removal is required. NAA requires successive layer removal and analysis to obtain any information on depth concentration profile. For both of these techniques, the sample is prepared in plan view as illustrated in Figure 13 and described below.

Prior to analysis, the oxide layer must be removed for either technique to be useful. The most straightforward means of removing this layer is via mechanical polishing. Care must be taken to remove the entire protective layer and none of the underlying metal, as the highest concentration of Ag will be located at the surface of the specimen. Further care must be taken that the sample is not heated during polishing as excessive heat may further diffuse Ag into the metal, making meaningful comparisons difficult. If the oxide layer can be removed via chemical processing, while leaving the underlying metal (and any Ag in the metal) undisturbed, this would be another acceptable means of preparation.

Mechanical polishing is a very simple way to prepare the specimen for either RBS or NAA analysis. However, a high level of accuracy during polishing is needed. A more serious disadvantage to this type of specimen preparation is that the protective oxide layer must be destroyed. If a high level of Ag is measured in the underlying metal, the protective nature of the layer must certainly be questioned. However, if the layer has been removed, it is impossible to determine whether this failure is due to the properties of the layer (composition, structure, etc.) or defects in the structure created during deposition.

Some composition profile information is possible using RBS and NAA via additional sample preparation steps. If successive layers of the metal matrix are removed, the composition can be measured at each thickness to yield composition profiles. Again, the depth resolution using successive layer removal is dependent on the thickness of the layers removed, ~1 micron.

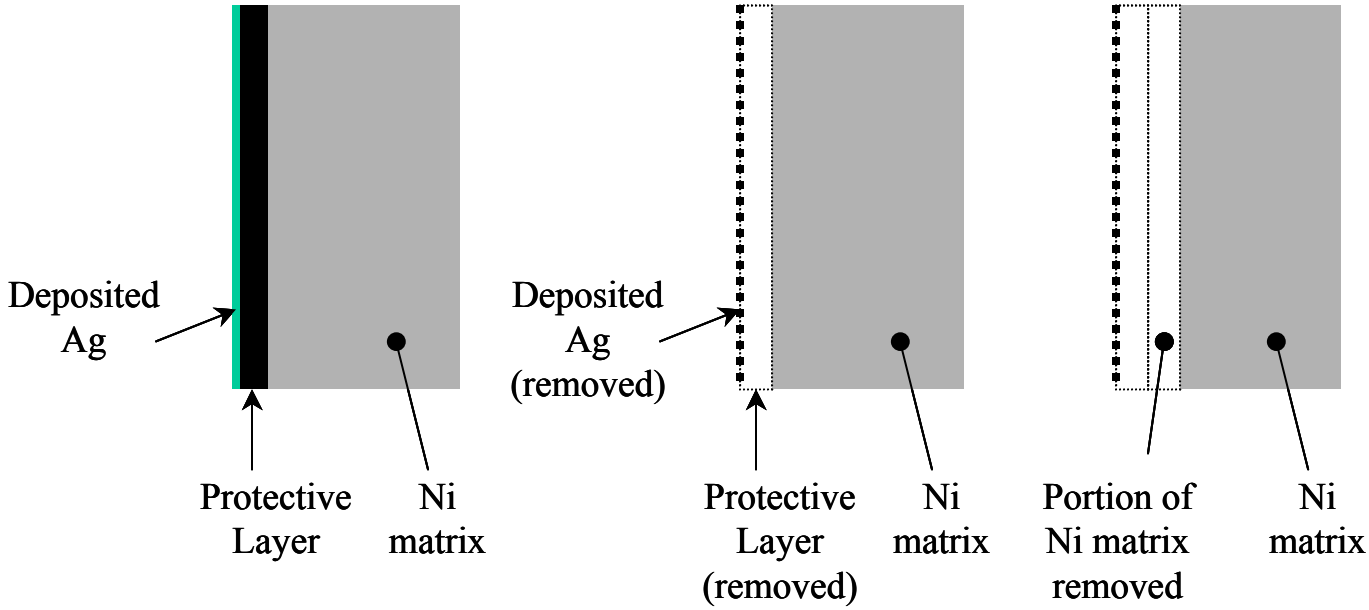

Figure 13: Schematic of specimen preparation for "plan view" geometry.

Reverse Plan View

Keeping the protective layer intact would be of great value in assessing the performance of the layer and identifying ways to improve that performance. Therefore, another means of specimen preparation would be beneficial. Unfortunately, for NAA, the oxide layer must be removed entirely for accurate results. However, for RBS, the sample may also be prepared in a "reverse plan view." This is illustrated in Figure 14.

In the reverse plan geometry, the underlying metal material is removed from the backside of the sample by mechanical polishing or a combination of mechanical and electropolishing. Again, care must be taken that the sample is not heated during polishing.

This approach does leave the protective layer intact and provide an opportunity to obtain composition profile data using RBS. However, such a procedure would be laborious and time consuming.

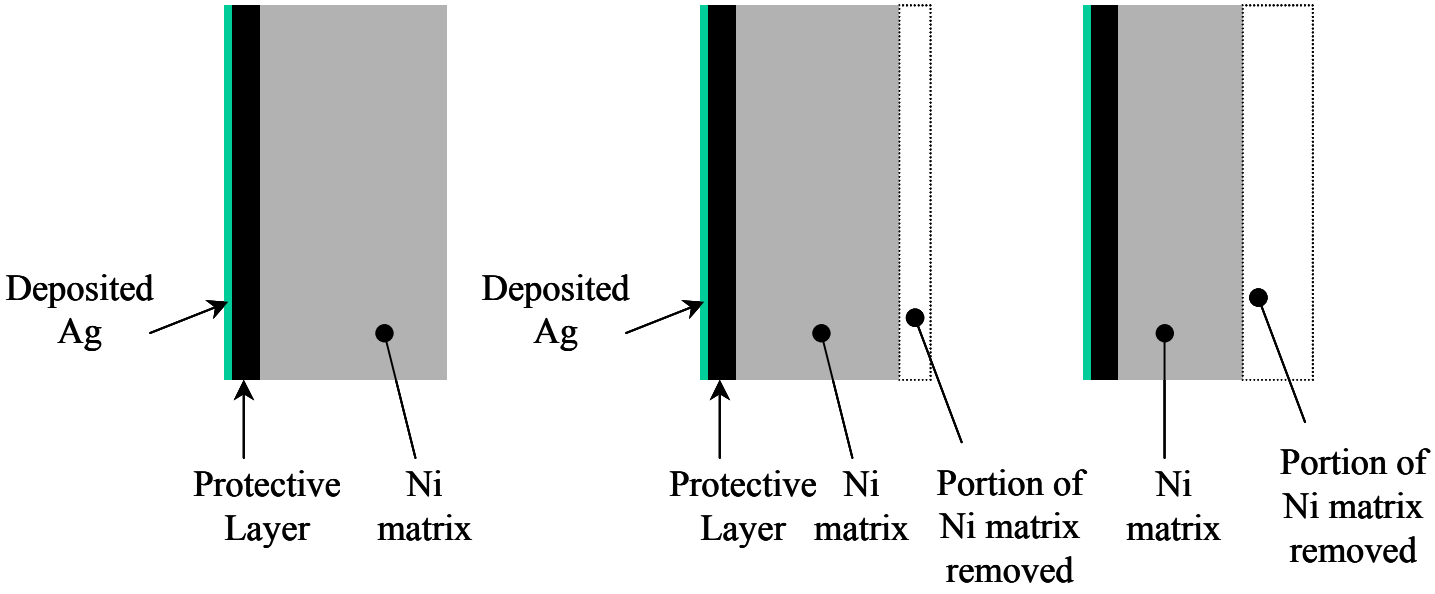

Figure 14: Schematic of "reverse plan view" specimen geometry.

Cross-sectional View

EMPA provides a high spatial resolution allowing for easy generation of compositional profiles. The composition of Ag can be readily determined as a function of depth in through the protective oxide layer, the oxide-metal interface, and the underlying Ni (or Inconel) substrate without any loss of elemental resolution if a cross-sectional sample is prepared. This is illustrated in Figure 15.

A cross-sectional specimen is prepared by cutting the specimen perpendicular to the plane of the interface. EMPA requires optically flat, stable specimens, so precision during cutting is required. As with mechanical polishing, care must be taken not to heat or deform the specimen during cutting. Low speed diamond saws are capable of making a high precision cut with minimal wastage of material and heat generation.

Leaving the protective layer intact is a clear advantage to cross-sectional specimen preparation. However, as both cutting and polishing are required the possibility of creating artifacts by heating the sample is increased.

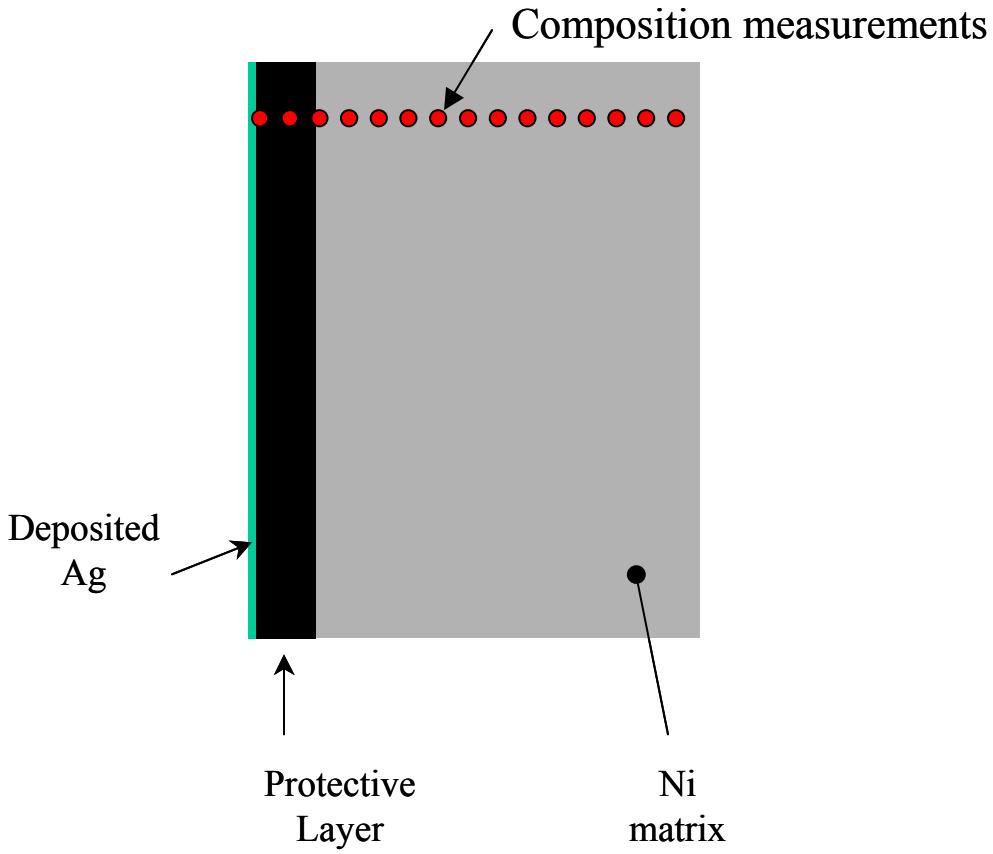

Figure 15: Cross-sectional specimen preparation geometry.

Summary and Recommendations

All three techniques can be used to determine the amount of Ag, which has diffused through the protective layer into the underlying metal. Each technique has distinct advantages and disadvantages that have been summarized for each technique. The three techniques are compared directly in Table 5. EMPA has the lowest elemental sensitivity, but is also the most straightforward technique with the simplest sample preparation, and provides fair depth resolution. NAA has the highest sensitivity, but requires that the oxide layer be removed, renders the sample radioactive and has the lowest depth resolution. RBS provides intermediate level of sensitivity but the best depth resolution.

It is also important to note that while the ultimate objective of the work is to develop coatings that resist diffusion of Ag-110m, it is not necessary to use radioactive isotopes for testing of these coatings, which creates the requirement that all test specimens must be handled as radioactive. Rather, non-radioactive isotopes of Ag can be used to simulate diffusion through the

barrier coating. Since the chemical interactions between the oxide and stable and radioactive isotopes are the same, diffusion rates will differ by the square-root of the ratio of masses. For Ag-110m and naturally occurring Ag, this results in less than a 1% difference in diffusion rate.

A final note should be made about the three different techniques and specimen geometries. These three techniques can be used in a complimentary fashion. Following heat treatment, a cross-sectional specimen can be cut, providing a sample for EMPA analysis and an archived specimen with the protective layer intact. The protective oxide layer can then be removed from the remainder of the specimen for RBS analysis. After RBS analysis, the sample could be used for NAA analysis.

Table 5: Comparison of different analysis techniques

	Sensitivity for Ag						
Technique	In pure Ni	In Inconel	Depth Resolution	Depth Profiling ?	Destructive ?	Sample Form	Time for analysis
RBS	20 appm	0.1 at%	36 nm up to 400 nm, 1 μm beyond	Y[2]	Y	Oxide removed	~ 1 hr
NAA	0.5 appm	0.5 appm	~1 μm	Y[2]	Y[3]	Oxide removed	~ 2 hr
EMPA	400 appm	400 appm	~1 μm[1]	Y	Y	X-section	~ 1/2 hr

[1]Depth resolution for EMPA refers to the distance from the protective layer/metal interface to remain consistent with RBS and NAA
[2]Depth profiling only available if successive layers are removed.
[3]Sample becomes radioactive.

References

[1] RUMP Program, Rutherford BackScattering Data Analysis Plotting and Simulation Package, Computer Graphic Service, El Paso, TX.
[2] SIMNRA Program, Ion Backscattering Simulation Program, Institut fur Plasmaphysik, Julich, Germany.
[3] IBA Analysis Program, J.F. Ziegler, IBM Corp., Yorktown, NY.
[4] P. Shewmon, "Diffusion in Solids," Published by The Minerals, Metals, and Materials Society, 1989.
[5] Atomic Defects in Metals, ed. H. Ullmain, Landolt-Bornstein, New Series, Group 3, Vol. 25 (Springer-Verlag, City, 1991).
[6] Reproduced from http://www.missouri.edu/~glascock/naa_over.htm
[7] Neutron Activation Calculator, http://www.antenna.nl/wise/uranium/rnac.html

[8] Image reproduced from http://jan.ucc.nau.edu/~wittke/Microprobe/ProbeIntro.html

APPENDIX A - TURBINE BLADE MATERIAL

The following information is taken directly from EPRI, "Evaluation of Materials Issues in the PBMR and GT-MHR", October 17, 2002

For the PBMR

High Pressure and Low Pressure Turbines (HPT and LPT)

Blades and Stator Vanes

The inlet temperatures to the HPT and LPT are approximately 900°C and 800°C, respectively. Thermal fluence should be $<2x10^{19}$ n/cm^2. The material chosen for the rotating blades is a MHI-proprietary designation, a Ni-base alloy containing about 10%Co for high temperature strength purposes. The stator vanes are to be of a similar Ni-base alloy, containing about 20% Co. These materials require no cooling for the design operating conditions, and provide associated benefits in terms of efficiency.

The specific identification of the MHI HPT alloy, 10%Co-Ni, is very "generic". There are numerous cast alloys with this basic composition, including the MarM247 alloy that was originally selected for the power turbine blades. These alloys typically contain 10-12%W, Ta and Nb in the 1 to 3% range (each), and Al and Ti ranging from 1 to 6% each. There are also a few wrought alloys in the general category of 10%Co-Ni. They typically contain W, Ta, or Nb and are not as strong as the cast materials. 20%Co-Ni is also a generic designation. There are wrought (Nimonic 263 and IN 597) and cast versions (MarM432) of 20%Co-Ni. Alloying additions are similar to those on the 10%Co-Ni alloys. They are typically a little stronger than the 10%Co variants up to about 750^{o}C.

Discs

The material selected for the turbine discs, cooled to ~500°C, is precipitation-hardenable Inconel 718. This wrought Ni-base alloy contains nominally 19%Cr, 18%Fe, 5%Nb+Ta, 3%Mo, 1%Ti and 0.5%Al, and is hardened by a solution treatment at 980°C, plus aging steps at 720°C and 620°C.

Casings

Casings are also cooled to ~500°C and the selected casing material is Hastelloy X, a well known and extensively used wrought Ni-base alloy. Its basic composition is 47%Ni, 22%Cr, 1.5%Co, 9%Mo, 0.6%W, 18.5%Fe, 0.5%Mn, 0.5%Si, and 0.1% C.

Rotors

The turbine rotors operate at 150°C. The selected material is Inconel 718 (See Section 2.2.2.4.2).

Component	Sub-Unit	Material	Damage Mechanisms Considered	Issues to be Resolved	Method of Resolution	Current PBMR Resolution Activities
HPT and LPT	Blades	10%Co-Ni alloy	Fatigue, thermal embrittlement and creep, He effects	Evaluate operational effects of coatings		
	Stator Vanes	20%Co-Ni alloy	As above	As above		
	Discs	Inconel 718	Fatigue	None		
	Casings	Hastelloy X	Fatigue	None		
	Rotors	Inconel 718	Fatigue	None		

For the GR-MHR

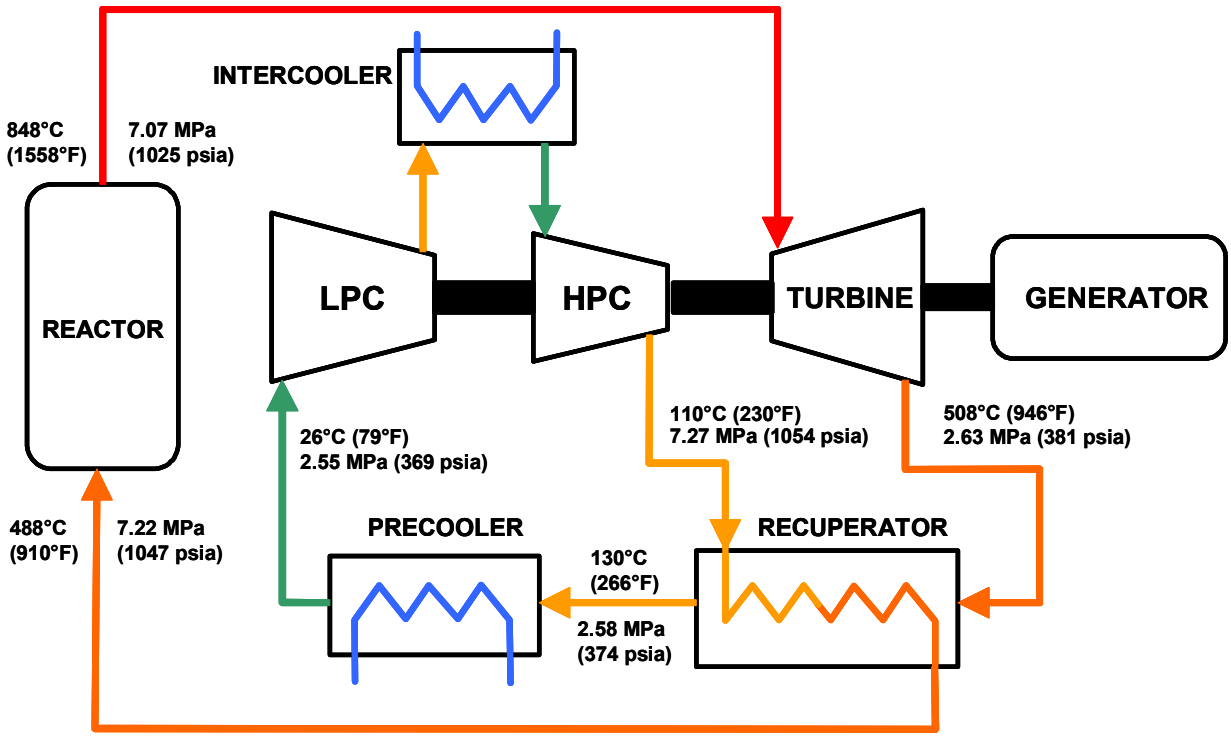

System	Component	Sub-Unit	Normal Operating Conditions			Off-Normal Conditions	Material
Power Conversion Unit (PCU)	Turbine	Blades	850°C	$7x10^{12}$[10]	He	890°C[11]	ZhS6[12]
		Disks	850°C	$7x10^{12}$	He	890°C	EI 698[12]
		Stator	850°C	$7x10^{12}$	He	890°C	ZhS6[12]
		Volute	850°C	$7x10^{12}$	He	890°C	VKL 14N[12]
	Compressors	Blades	110°C	$4.7x10^{12}$/ $1.4x10^{12}$ HPC/LPC	He	200°C[11]	VT6 titanium alloy
		Disks	110°C	$4.7x10^{12}$/ $1.4x10^{12}$ HPC/LPC	He	200°C	VT6 titanium alloy
		Stator	110°C	$4.7x10^{12}$/ $1.4x10^{12}$ HPC/LPC	He	200°C	10Cr18Ni9NbBe

Turbomachine

Fatigue and creep are the most important damage mechanisms for the first few stages of the turbine blades and disks. The material issue/requirement is to ensure the sufficiency of fatigue and creep strengths to allow the desired design lifetime of seven years. The proposed method of resolution is the selection of the materials and coatings. A preliminary selection of the materials has been made as shown in Table 3-1. OKBM has started a technology development program funded by the International Science and Technology Center (ISTC) to verify these selections.

APPENDIX B – COATING EQUIPMENT MANUFACTURERS, INSTITUTES AND APPLICATORS

Equipment Manufacturers

There are a number of eb-PVD equipment suppliers active in the European market. These include Von Ardenne, ALD and the Paton Institute. For VPS/LPPS there are now only two supply companies. These are Sulzer Metco and Medicoat.

Von Ardenne

This company is based in Dresden, Germany. They have been very active in system sales and have a joint venture with a Dutch company Interturbine (see below). Their contact details are listed below.

Von Ardenne
Dresden - Weisser Hirsch
Plattleite 19/29
D-01324 Dresden
Germany

Contact Name: Carsten Deus

tel +49 (0) 351/26 37- 3 00
fax +49 (0) 351/26 37- 3 08
email: office@ardenne-at.de
web url: http://www.ardenne-at.de/enhome/home.htm

ALD
This German company has been very active in Europe and the US. I spoke with Jürgen Hotz (tel: 49 61813073227 email: Juergen.Hotz@ald-vt.de. They do not have a test facility in house and had no direct, hands-on experience of coating oxides except zirconia.
As far as capability was concerned, the systems supplied to date had been for aero-engine blades ie small components. However, they have just supplied one into the US market capable of coating IGT parts.
They also have offices in the UK and the USA.

Dr. Rainer Schumann
ALD Vacuum Technologies, Inc.
18 Thompson Road
East Windsor, CT 06088
Tel.: +1 (860) 3 86 72-27

Fax.: +1 (860) 3 86 72-20
e-mail: rschumann@ald-usa.com

Mr. Philip Wightman
ALD Vacuum Technologies, Ltd.
The Frensham Suite
13-21 High Street
Guildford, Surrey GU13DG
Tel.: +44 (1483) 45-4434
Fax.: +44 (1483) 30-6641
e-mail: ald.vactech@btclick.com

EO Paton Institute

They have built a number of small pilot plant equipment which may be found in a number of labs and companies (eg Interturbine's first eb PVD machine was from Paton0. I'm not sure how commercial they are and whether there are any/many of their systems in production. Note that Penn State have one.

Institutes

There are a number of institutes actively investigating both eb PVD and VPS/LPPS. I know both Cranfield and DLR and found the Penne State group on the web.

Cranfield, UK

Prof John Nicolls (tel: 44 1234 754039 email: j.r.nicholls@cranfield.ac.uk) has just purchased an eb-PVD machine together with a large VPS/LPPS system. They plan to be able to coat real/large components and to develop new coatings for industry. They were very interested in the MgO-Al2O3 system as offering improved strain tolerance for TBC's on blades.
DLR, Germany
They have a small ALD lab system but- have been working on non-zirconia ceramics.
Contact: Dr. U.Schulz (tel. +49 2203 601 2543 e-mail uwe.schulz@dlr.de)

PENN STATE EB-PVD CONSORTIUM

Dr. J. Singh
(814) 863-9898
jxs46@psu.edu
The purpose of the Electron Beam–Physical Vapor Deposition Consortium at ARL Penn State is to assist in the development and commercialization of advanced EB–PVD coating technology. A key element of our mission is the advancement of EB–PVD coating technology using the Paton Welding Institute (PWI) multiple ingot industrial coater. By leveraging U.S. Navy Mantech

development of new coatings with technology transfer of PWI coatings, consortium members will share resources and results for new coating fabrication technology.

Coating Companies

There are many companies with VPS/LPPS systems in the market but relatively few with eb PVD capabilities. I have listed the thre most well know outside the OEM companies.

Interturbine Coating Center BV
Spikweien 44
NL-5943 AD Lomm, Netherlands
Telephone: +31 77 4738474
Fax: +31 77 4738472
Internet: www.itcoating.nl

Located in Lomm, The Netherlands this company is now owned by Sulzer. I spoke with their technical manager Geil Marijnissen They have a joint venture with and operate a Von Ardenne eb PVD system but only have experience of depositing zirconia TBC's. In principal there is no problem in coating other ceramics but this would have to fit in with production loads.

Howmet

Thermatech Coatings
555 Benston Road
Whitehall, MI 49461-1899
Telephone: (231) 894-7436
Fax: (231) 894-7400
http://www.howmet.com

Coaters of both aerospace and power gen components with most industry approvals.

They have the following facilities:

• Chemical Vapor Deposition (CVD)
• CVD-aluminide, noble-metal aluminide and silicon aluminide. Various units with a working zone of up to 40 inches in diameter x 50 inches in length.
• Pack cementation - noble-metal aluminide, aluminide, chromium
• Plasma spray: low-pressure, high-velocity oxy-fuel (HVOF) and air
• Electron Beam Physical Vapor Deposition (EBPVD)
• Vacuum brazing
• Vacuum heat treat
• Part stripping

From the web they say "Howmet Thermatech Coatings has been providing sophisticated coating services to the aerospace and power generation industries since 1963. The advanced coatings supplied by Thermatech are designed to extend the operating life of the most complex components by providing them with the highest degree of protection against the damaging effects of oxidation and corrosion. Thermatech Coatings specializes in the coating of hot-section components cast in nickel-based alloys with equiax, directional solidification and single crystal orientation."

Chromalloy

Chromalloy have a jv with Rolls-Royce in the UK and have one installed and one system about to be installed near Derby. The contact is Dr David Rickerby. In the US they have a large facility in Arizona.

Chromalloy Arizona
5161 West Polk Street
Phoenix, Arizona 85043
Main Phone: (602) 272-1768 Main Fax: (602) 233-3347

They have the following coating processes:

Diffused Aluminide (pack and gas phase methods)
Diffused Chromium Aluminide (pack method)
Diffused Platinum Aluminide (pack, gas phase, and CVD methods)
Diffused Rhodium-Platinum Aluminide for Cobalt Alloys (pack method)
Diffused Silicon Aluminide (pack method)
Electron Beam Physical Vapor Deposited Coatings: *
CoCrAlY Overlay Coating Class I (RT-30)
CoNiCrAlY Overlay Coating Class II (RT-31)
NiCoCrAlY Overlay (RT-270)
Yttrium Stabilized Zirconium Thermal Barrier
Coating Class III (RT-33)

- Turbine Airfoil Coating and Repair, New York

APPENDIX – C – COATINGS GLOSSARY

Further surface engineering terms may be found at this site:
http://www.btinternet.com/~catechnology/surfaceweb/swebinfopage_files/glossary.htm

Abrasive blasting
A pressurised stream of hard metal or oxide grit material used to clean and/or roughen surfaces prior to coating.

Alumina
Aluminium Oxide compound used in both abrasive blasting as an abrasive and in thermal spraying as a consumable feedstock (powder and rod) for the production of coatings. Alumina is a hard wear resistance ceramic and can be alloyed with various amounts of titania (titanium dioxide) to improve certain properties.

Aluminising (gas)
High temperature (approx 900oC) pack or gaseous diffusion of aluminium into the surface of a component to enhance high temperature corrosion and oxidation resistance.

Bond
This represents the state of adhesion between the coating and the substrate. It's strength will depend on the details of the spraying process and the materials used. Bonding mechanisms may be mechanical, physical or metallurgical or a combination of these.

Bond coat
A coating applied as an intermediary between the main or top coating and the substrate in order to improve the bond strength.

Bond strength
The strength of the adhesion between the coating and the substrate. A number of test methods are in use to measure the bond strength of coatings.

Chemical Vapour Deposition (CVD)
The deposition of a coating by means of a chemical reaction in gases in a chamber producing components which deposit on and adhere to the substrate.

Coating
The application of a thin (generally less than 1mm) layer of material onto the surface of a substrate.

Corrosion
Chemical or electrochemical reaction between a metal and the local environment whether wet or dry which results in deterioration in the properties of the metal.

Grit blasting
A pressurised stream of hard metal or oxide grit material used to clean and/or roughen surfaces prior to coating.

Ion-Implantation
A process in which a beam of positive ions is projected towards and into the surface. It is carried out in partial vacuum and the ions diffuse into the surface layer of the substrate. Typically this is carried out with nitrogen giving a nitrided effect.

Ion Plating
The deposition of metals by a vacuum evaporative process.

LPPS
See 'Vacuum Plasma Spraying.'

MCrAlY
MCrAlY's (where M = Ni, Co or Fe) are a group of high temperature, corrosion resistant alloys used to combat sulphidation and oxidation.

Mechanical bonding
Usually represented by mechanical interlocking of the deposited particles with the rough heights on the substrate surface produced during grit blasting.

Oxidation
Chemical reaction between the surface elements and oxygen causing oxides of the elements to be formed.

Oxidising
The production of a stable oxide layer on a steel component by heating in a controlled atmosphere. Provides corrosion protection and reduced friction.

Physical Vapour Deposition
A term covering all the vapour deposition processes including Ion plating, It does not include CVD as this is chemical not physical.

Plasma
Plasma is a gas (usually Argon, Helium, Nitrogen, Hydrogen) that has been heated to a sufficiently high temperature to become partially ionized and therefore electrically conductive. The term was introduced by Irving LANGMUIR in 1930.

Plasma Spraying
A thermal spraying process in which the heat source is a plasma jet.

Shot peening
The bombardment of a component surface with steel or cermamic shot. Produces a residual compressive stress in the surface and improves fatigue and stress corrosion performance.

Silver plating
The electrodeposition of silver for electrical, decorative or anti-fretting properties.

Spray chamber
A chamber in which the spraying process is carried out. It may merely be an acoustic chamber for plasma spraying or a vacuum chamber for vacuum plasma spraying.

Sputtering
This is a glow discharge process whereby bombardment of a cathode releases atoms from the surface which then deposit onto a nearby target surface to form a coating.

Strain
A measure of the extent to which a body is deformed when it is subjected to a stress.

Stress
The force per unit area on body that tends to cause it to deform. It is a measure of the internal forces in a body between particles of the material of which it consists as they resist separation, compression, or sliding.

Surface energy
Surface energy exists because the molecules of a condensed phase are atttracted to each other, which is what causes the condensation. The force required for the removal of molecular contact from above a surface, i.e. for the bond-breaking, is the surface energy.

Surface preparation
Cleaning and roughening the surface to be sprayed, usually by grit or bead blasting. This is to increase the adhesion of the coating to the substrate.

Thermal barrier coating
A coating produced to present an insulating barrier to a heat source and to protect the substrate.

Vacuum or Low Pressure Plasma Spraying
Plasma spraying carried out in a chamber which has been evacuated to a low partial pressure of oxygen. It is then usually partially backfilled with argon to avoid the possibility of forming a glow discharge.

About EPRI

EPRI creates science and technology solutions for the global energy and energy services industry. U.S. electric utilities established the Electric Power Research Institute in 1973 as a nonprofit research consortium for the benefit of utility members, their customers, and society. Now known simply as EPRI, the company provides a wide range of innovative products and services to more than 1000 energy-related organizations in 40 countries. EPRI's multidisciplinary team of scientists and engineers draws on a worldwide network of technical and business expertise to help solve today's toughest energy and environmental problems.

EPRI. Electrify the World

1009385

Printed on recycled paper in the United States of America

EPRI • 3412 Hillview Avenue, Palo Alto, California 94304 • PO Box 10412, Palo Alto, California 94303 • USA
800.313.3774 • 650.855.2121 • askepri@epri.com • www.epri.com